JCB Journal of Cell Biology

ARTICLE

Mechanosensitive collaboration between integrins and connexins allows nutrient and antioxidant transport into the lens

Jie Liu[1,2], Manuel A. Riquelme[1], Zhen Li[1], Yuting Li[1], Yuxin Tong[1], Yumeng Quan[1,2], Cheng Pei[2], Sumin Gu[1], and Jean X. Jiang[1]

The delivery of glucose and antioxidants is vital to maintain homeostasis and lens transparency. Here, we report a new mechanism whereby mechanically activated connexin (Cx) hemichannels serve as a transport portal for delivering glucose and glutathione (GSH). Integrin α6β1 in outer cortical lens fiber activated by fluid flow shear stress (FFSS) induced opening of hemichannels. Inhibition of α6 activation prevented hemichannel opening as well as glucose and GSH uptake. The activation of integrin β1, a heterodimeric partner of α6 in the absence of FFSS, increased Cx50 hemichannel opening. Hemichannel activation by FFSS depended on the interaction of integrin α6 and Cx50 C-terminal domain. Moreover, hemichannels in nuclear fiber were unresponsive owing to Cx50 truncation. Taken together, these results show that mechanically activated α6β1 integrin in outer cortical lens fibers leads to opening of hemichannels, which transport glucose and GSH into cortical lens fibers. This study unveils a new transport mechanism that maintains metabolic and antioxidative function of the lens.

Introduction

The lens is a unique avascular and transparent organ whose primary function is to transmit and focus light on the retina. Lens transparency relies on an effective delivery of nutrients and antioxidants to the distinctly different metabolic regions of the lens (Braakhuis et al., 2019). A relatively high level of reduced glutathione (GSH) is required to protect lens fibers against oxidative stress. Glucose that produces NADPH through the pentose phosphate pathway aids in maintaining the high levels of GSH (Giblin, 2000). Microcirculation is suggested to be a major driving force for delivery of nutrients, metabolites, and antioxidants to the lens (Donaldson et al., 2010; Mathias et al., 2007, 2010). However, the precise underling mechanism of how microcirculation promotes glucose and antioxidant distribution remains unclear. Elucidation of the molecular mechanism governing glucose and antioxidants distribution will help develop therapeutic strategies for treating cataracts, the leading cause of blindness in the world.

Two connexins, Cx50 and Cx46, are predominantly expressed in lens fiber cells. Mutations of either connexin is directly linked to human congenital cataracts. In addition to cataract formation, Cx50 knockout (KO) mice develop microphthalmia, suggesting a unique role of Cx50 in lens development (Jiang, 2010). However, the precise mechanism of how connexins regulate lens growth and protect against cataract formation remains elusive. Connexin hemichannels at the cell surface mediate communication between cells and the extracellular environment by rapid exchange of ions, second messengers, and metabolites (<1 kD; Beyer and Berthoud, 2014; Fasciani et al., 2013). Active Cx50 hemichannels are shown to protect lens cells against oxidative damage (Shi et al., 2018). However, the specific role of connexin hemichanels on lens fibers in maintaining lens transparency is largely unknown. Hemichannels formed by Cx43 are shown to be permeable to GSH and glucose (Niu et al., 2016; Retamal et al., 2007; Slavi et al., 2014). These findings have prompted the consideration of connexin hemichannels in the lens fibers as a potential transport portal for glucose and antioxidants.

Hemichannel opening is tightly regulated by multiple factors, including mechanical loading (Batra et al., 2012; Trexler et al., 1999; Wang et al., 2012). In the lens, connexin hemichannels on the surface of fiber cells are subjected to fluid flow shear stress (FFSS) applied by mechanical loading, which is caused by lens accommodation, and constitutive microcirculation of fluid initiated by a sodium gradient across the lens epithelial cell membrane (Mathias et al., 2007). However, the specific molecular mechanism governing lens connexin hemichannel opening

[1]Department of Biochemistry and Structural Biology, University of Texas Health Science Center, San Antonio, TX; [2]The First Affiliated Hospital of Xi'an Jiaotong University, Xi'an, China.

Correspondence to Jean X. Jiang: jiangj@uthscsa.edu.

under mechanical stimulation remains elusive. The fact that integrins participate in mechanotransduction has been reported in other systems (Davis et al., 2001; Ross et al., 2013). Shear stress has been shown to activate integrin β1 and its downstream kinase signaling pathway in endothelial cells (Katsumi et al., 2004). In addition, integrin α5β1 is evidenced to mediate Cx43 hemichannel opening under shear stress in bone osteocytes (Batra et al., 2012). Various subtypes of integrins are expressed in the lens, and most of them are strictly expressed in lens epithelial cells (Walker and Menko, 2009). While integrin α6β1 is expressed in both the lens epithelial and outer cortex of lens fiber cells, the presence of integrin α6β1 along the long cell–cell borders of nascent fiber cells (Walker and Menko, 2009) indicates that this integrin could be a candidate for being activated by mechanical stimuli and subsequently induce the opening of lens connexin hemichannels.

In this study, we investigate the role of connexin hemichannels in lens glucose and GSH delivery, and the molecular mechanism governing hemichannel opening under mechanical stimulation. We show that integrin α6β1 serves as a mechanosensitive component, and activation of the integrin by FFSS leads to the opening of hemichannels in lens cortical fibers through its interaction with the C-terminus of Cx50. Hemichannel opening from mechanical stimuli did not occur in central nuclear fiber cells in the absence of integrin and C-terminal truncation of Cx50. Furthermore, the activation of hemichannels by FFSS serves as a portal for the influx of glucose and GSH into cortical fiber cells. These results provide insight into how glucose and antioxidants are efficiently transported by lens microcirculation and identify connexin hemichannels and integrin α6β1 as important players in maintaining lens homeostasis and transparency.

Results

Mechanical stress increases connexin hemichannel activity in differentiated lens culture

Differentiated primary chicken lens culture forms lentoid structures with characteristics that mimics differentiating lens fibers in vivo (Jiang et al., 1993; Menko et al., 1984). These lentoid structures are able to form hemichannels and gap junctions composed of Cx50 and Cx46. To test hemichannel opening, ethidium bromide (EtBr) and FITC-dextran dye uptake assay was used after FFSS stimulation. EtBr (M_r 394 D) is permeable to hemichannels and is retained inside the cell by binding to DNA, which prevents it from passing through gap junctions. The large FITC-dextran (M_r ~10 kD) is unable to pass through hemichannels and served as a control for nonspecific, permeable, dying cells. Differentiated primary chick lens cell culture was subjected to FFSS at 1 dyn/cm^2, which is comparable to the physiological level of shear stress estimated in vivo (Fischbarg et al., 1999). FFSS significantly increased EtBr uptake in lentoids compared with the unloaded group (Fig. 1 A). The increased EtBr uptake in lentoids was blocked with an exogenously expressed dominant-negative mutant, Cx50 (P88S), which prevents hemichannel opening (Banks et al., 2007). EtBr uptake in lentoids of primary lens culture was also inhibited with flufenamic acid, a chemical inhibitor for Cx50 and Cx46 hemichannels (Srinivasan et al., 2002), or niflumic acid (NA), an inhibitor for Cx50 hemichannels (Eskandari et al., 2002; Fig. 1 B, upper panel). The protein expression of the endogenous Cx50 and exogenous P88S was determined by immunoblot (Fig. 1 B, lower panel). Exogenous Cx50 P88S mutant was FLAG tagged, resulting in a slightly slower migration on SDS-PAGE compared with endogenous Cx50. These results demonstrate that connexin hemichannels are activated in lens fibers under FFSS.

Cx50 and Cx46 coexist in lens fibers and differentiated primary chick lens cell culture. We used a chicken embryonic fibroblast (CEF) cell model to individually characterize Cx hemichannels (Banks et al., 2007). Exogenous lens connexins and their mutants were introduced by retroviral infection. To determine the effect P88S has on channel function, we tested CEF cells expressing exogenous Cx50, Cx46, P88S, or combinations (P88S + Cx50 or P88S + Cx46; Fig. 1 C, left). The cells were mechanically stimulated by FFSS, and dye uptake assay was performed with Lucifer yellow (LY; M_r ~457 D) and rhodamine-dextran (RD). RD (M_r ~10 kD) was used to detect nonspecific uptake from dead, permeable cells. The percentage of dye uptake was quantified by LY-positive cells with the exclusion of LY/RD double-positive cells (Fig. 1 C, right). The hemichannels formed by either Cx50 or Cx46 were responsive to mechanical stimuli. Coexpression of either Cx50 or Cx46 with P88S ablated the hemichannel function of WT Cx50 and Cx46. To further confirm the data of FFSS, we applied mechanical stress by fluid dropping from a fixed distance. Fluid dropping showed similar effects of connexins and the P88S mutant on hemichannel opening compared with FFSS (Fig. S1). LY/RD were used in a CEF cell dye uptake assay, which had less background uptake than EtBr/FITC. LY can also be transported by gap junctions between cells. Thus, CEF cells were cultured at a low cell density to minimize the formation of gap junctions. These results suggest that hemichannels formed by Cx50 or Cx46 are responsive to mechanical loading in CEF cells.

Integrin α6β1 regulates hemichannel opening in response to mechanical loading

Previous studies report that integrin α6β1 is richly expressed in lens epithelial and nascent cortical fibers, the region where full-length Cx50 is expressed (Walker and Menko, 2009). This was confirmed in isolated chick lens portions containing cortical fibers or nuclear fibers. Crude membrane extracts were prepared from these lens portions, as well as from CEF cells and differentiated primary chick lens cell cultures. Integrin α6 was detected in cortical fibers, CEF cells, and differentiated primary chick lens cell culture with lentoids, but not in central nuclear lens fibers. Crude membrane extracts from whole chick lenses were loaded as a positive control (Fig. S2, A and B). The presence of integrin α6 in differentiated primary chick lens cell culture and CEF cells permitted us to adopt these cell models to study the regulatory mechanism of integrin α6β1 in hemichannel activity. The localization of integrin α6 and connexins in the lens was determined by dual immunolabeling of embryonic day 18 mouse lenses. Immunostaining of sagittal sections showed the expression of integrin α6, Cx50, and Cx46 in the lens (Fig. 2 A). Integrin

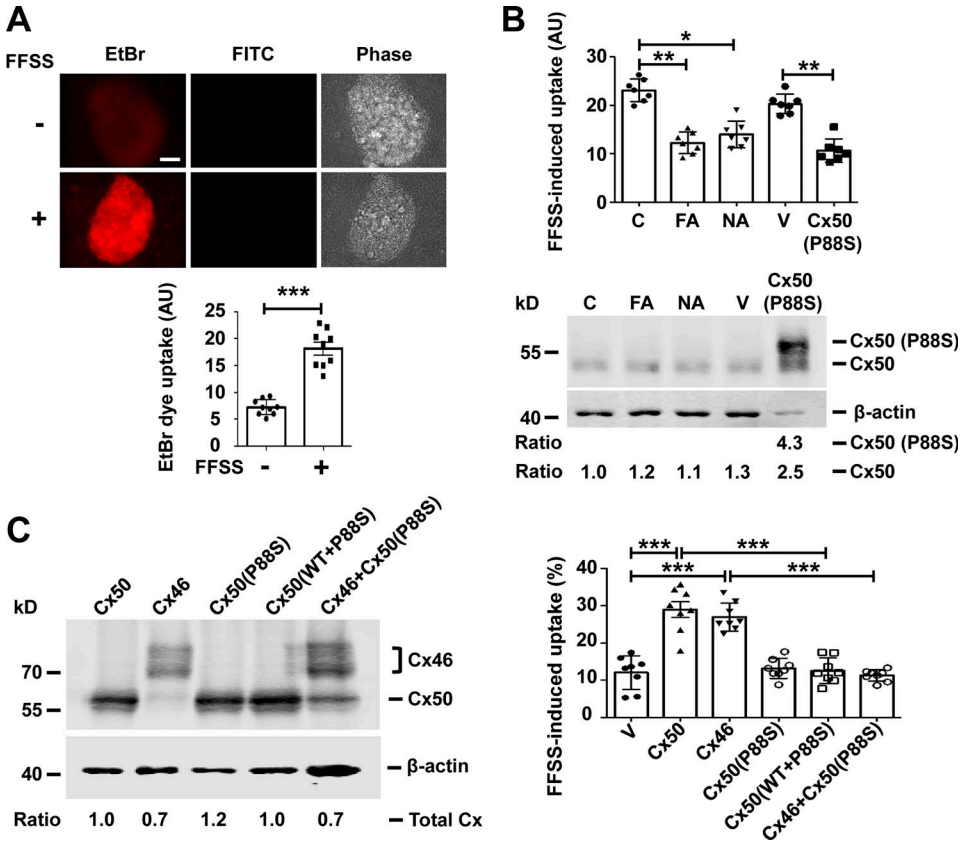

Figure 1. **Cx50 hemichannels are induced open by mechanical stress. (A)** Differentiated chick lens primary culture was subjected to FFSS, and EtBr/FITC-dextran dye uptake assay was performed and imaged (upper panel). Scale bar, 50 µm. FITC-dextran (M_r ~10 kD) is too large to pass through hemichannels in live cells and served as a control for nonspecific permeable, dying cells. The level of EtBr uptake in lentoids was quantified (excluding cells that took up both EtBr and FITC-dextran) using ImageJ (lower panel). Each data point in the graph represents an individual lentoid in one of three independent experiments. **(B)** Differentiated chick lens primary culture was treated in the absence (C) or presence of 100 µM flufenamic acid (FA) or 100 µM NA for 30 min or infected with high-titer RCAS(A) vehicle (V) or recombinant RCAS(A) retroviruses containing Cx50 mutant P88S. An EtBr uptake assay was performed after 10 min of FFSS at 1 dyn/cm^2 (upper panel). Each data point in the graph represents an individual lentoid in one of three independent experiments. Crude cell membrane extracts were immunoblotted with anti-Cx50 loop domain antibody and β-actin antibody (lower panel). The expression of Cx50 in the lentoids was quantified, and the relative ratio of band intensity of Cx50 to housekeeping protein β-actin with the ratio of the control set as 1 is shown underneath the immunoblot. **(C)** CEF cells were infected with high-titer recombinant RCAS(A) retroviruses containing Cx50, Cx46, or P88S or coinfected with P88S and Cx50 or Cx46. Crude cell membrane extracts were prepared and immunoblotted with anti-FLAG tag and β-actin antibody (left). The expression of retrovirus-induced exogenous connexins in the CEF cells was quantified. The relative ratio of band intensity of total connexins (Cx50 and/or Cx46) to housekeeping protein β-actin with the ratio of the control set as 1 is shown underneath the immunoblot. LY/RD-dextran dye uptake was conducted after FFSS. RD-dextran (RD; M_r ~10 kD) served as a control for nonspecific permeable, dying cells. The percentage of cells with LY dye uptake (excluding cells that took up both LY and RD-dextran) per image was quantified (right). Each data point in the graph represents an individual quantified image in one of three independent experiments. All data are presented as mean ± SEM. *, P < 0.05; **, P < 0.01; ***, P < 0.001.

α6 was colocalized with Cx50 in lens anterior epithelial cells (Fig. 2 B) and in lens equatorial epithelial and nascent fiber cells (Fig. 2 C). Cx46 colocalized with integrin α6 only at the equator lens regions and in nascent fiber cells, but not in lens epithelial cells (Fig. 2, B and C). These results are consistent with the absence of Cx46 in lens epithelial cells reported previously (Jiang et al., 1995). The colocalization between integrin α6 and Cx50 was strongest in equatorial epithelial and nascent fiber cells and decreased toward the central nuclear lens fiber region (Fig. 2 D). Our results suggest a close relationship between integrin α6 and lens Cx50 and Cx46.

The high degree of colocalization of Cx50 and Cx46 with integrin α6 led us to ask whether integrin α6 and integrin β1 (a known heterodimeric partner of α6) could participate in the opening of hemichannels as a mechanosensitive component under FFSS. Differentiated primary chick lens cell culture was exposed to FFSS and/or integrin β1-activating antibody-TS2/16 (β1 Ab; Jeong et al., 2018; Tsuchida et al., 1997). The treatment of β1 Ab induced the opening of hemichannels comparable to that of FFSS, indicated by EtBr uptake. To determine whether integrin β1 and FFSS work under the same mechanism in activating hemichannels, we treated primary chick lens cell culture with β1 Ab first and followed with FFSS stimulation. The results showed that β1 Ab and FFSS stimulation in combination did not have any additive effect in hemichannel opening compared with FFSS stimulation (Fig. 3 A). In contrast, treatment with integrin α6 inhibitory antibody (α6 Ab) prevented the activation of Cx hemichannels induced by FFSS. To determine whether integrin

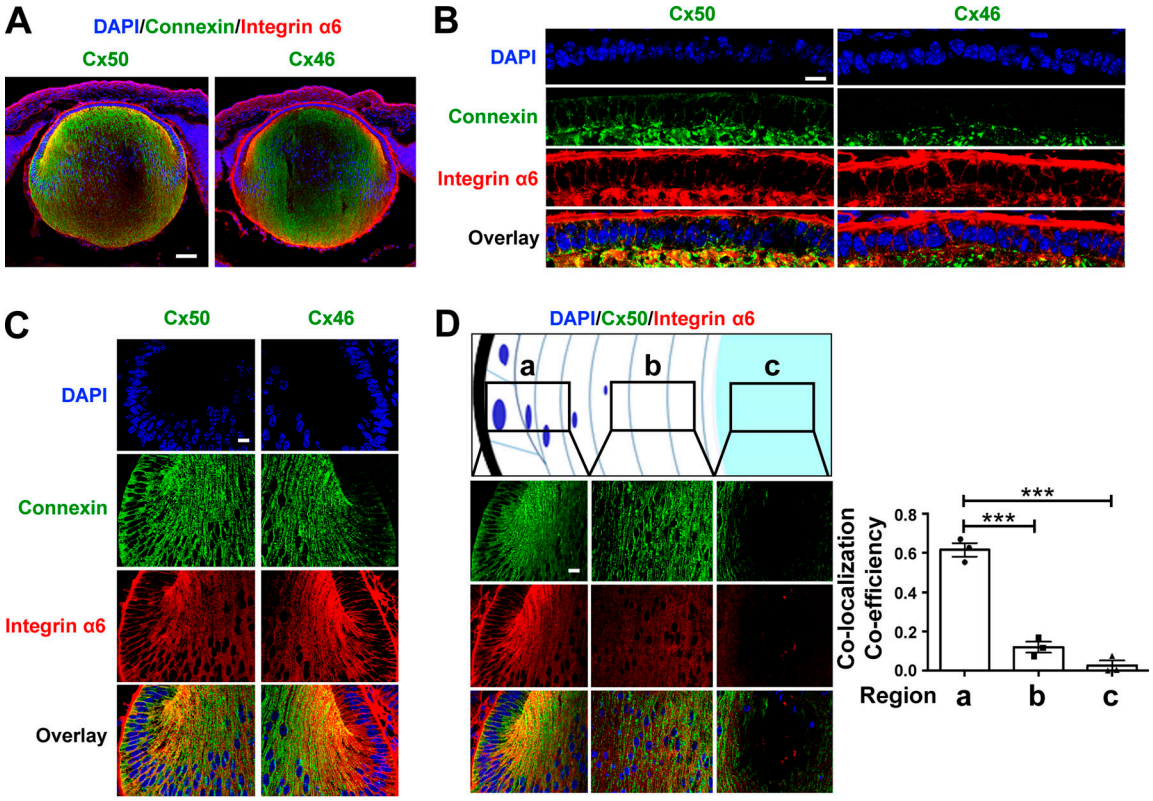

Figure 2. **Cx50 colocalized with integrin α6 in lens epithelium and outer cortical fiber cells. (A)** Embryonic day 18 mouse lens sagittal cryosections were immunostained with anti-Cx46 (green), Cx50 (green), or integrin α6 (red) antibody and counterstained with DAPI (blue), followed by corresponding secondary antibodies conjugated with either Alexa Fluor 488 or rhodamine. The corresponding images were merged (Overlay). Scale bar, 100 µm. **(B and C)** Anterior epithelial cells (B) and equatorial epithelial and nascent fiber cells (C). Scale bar, 20 µm. **(D)** Different depths of the lens regions from equator as illustrated in panels a (equator), b (cortical), and c (nucleus), Cx50 and integrin α6 were double immunostained (left), and the extent of colocalization was quantified and presented as colocalization coefficiency using ImageJ (right). Thick black outline indicates the lens capsule. Scale bar, 20 µm. Each data point in the graph represents an individual mouse in each group. The data are presented as mean ± SEM. ***, P < 0.001.

α6 activation is required in β1 Ab–induced hemichannel opening, we first treated differentiated primary chick lens cell culture with anti–α6 Ab, followed by treatment with β1 Ab. The results showed that dye uptake induced by β1 Ab was blocked by α6 Ab (Fig. 3 B). These data suggest that the opening of Cx50 hemichannels induced by activation of β1 integrin requires the activation of α6 integrin, which further supports the formation of a heterodimer by α6 and β1 integrins. We showed that Cx50 also colocalized with integrin α6 in lens epithelial cells. To further determine if a similar mechanoactivation mechanism also applied to hemichannels in lens epithelial cell, we subjected lens primary culture to FFSS, β1 Ab, or α6 Ab individually or in combination. An EtBr uptake assay was performed after the treatments. The results show that, similar to the observation in lentoids, FFSS or β1 Ab increased dye uptake in lens epithelial cells, and there was no additive effect if combination with FFSS and β1 Ab. α6 Ab decreased dye uptake induced by FFSS or β1 Ab (Fig. S3). Taken together, these data suggest that integrin α6β1 is required in FFSS-induced opening of hemichannels.

Because differentiated lens primary cultures coexpress Cx50 and Cx46 similarly to in lens cortical fibers, it is important to determine which connexin-formed hemichannels are regulated by integrin α6β1 under mechanical stress. To characterize Cx46 and Cx50 hemichannels separately, connexins were individually expressed in CEF cells by RCAS(A) retrovirus containing Cx50 or Cx46. Fluid dropping was applied to CEF cells, and hemichannel opening was assessed by LY/RD uptake. The results show that Cx50 hemichannels are stimulated by fluid dropping and β1 Ab. However, Cx46 hemichannels were induced open only by fluid dropping, but not β1 Ab, suggesting that Cx46 hemichannels are not directly regulated by integrin activation (Fig. 3 C). Moreover, α6 Ab significantly reduced Cx50 hemichannel opening under fluid dropping (Fig. 3 D). These data suggest that hemichannels formed by Cx50, but not Cx46, are regulated by integrin α6β1 in response to mechanical stimulation.

Cx50 and Cx46 form heteromeric hemichannels in lens fibers (Jiang and Goodenough, 1996). To test if integrin α6β1 is involved in the regulation of heteromeric hemichannel opening, CEF cells coinfecting with Cx50 and Cx46 was used. Crude membrane extracts containing Cx46, Cx50, and P88S, individually or in combination, were immunoblotted (Fig. S4 A). An LY/RD uptake assay was conducted after β1 Ab treatment (Fig. 4 A). Dye uptake analysis showed that β1 Ab increased dye uptake in Cx50/Cx46-coinfected CEF cells, and this increase was not observed in cells expressing Cx46 alone or in combination with the P88S mutant

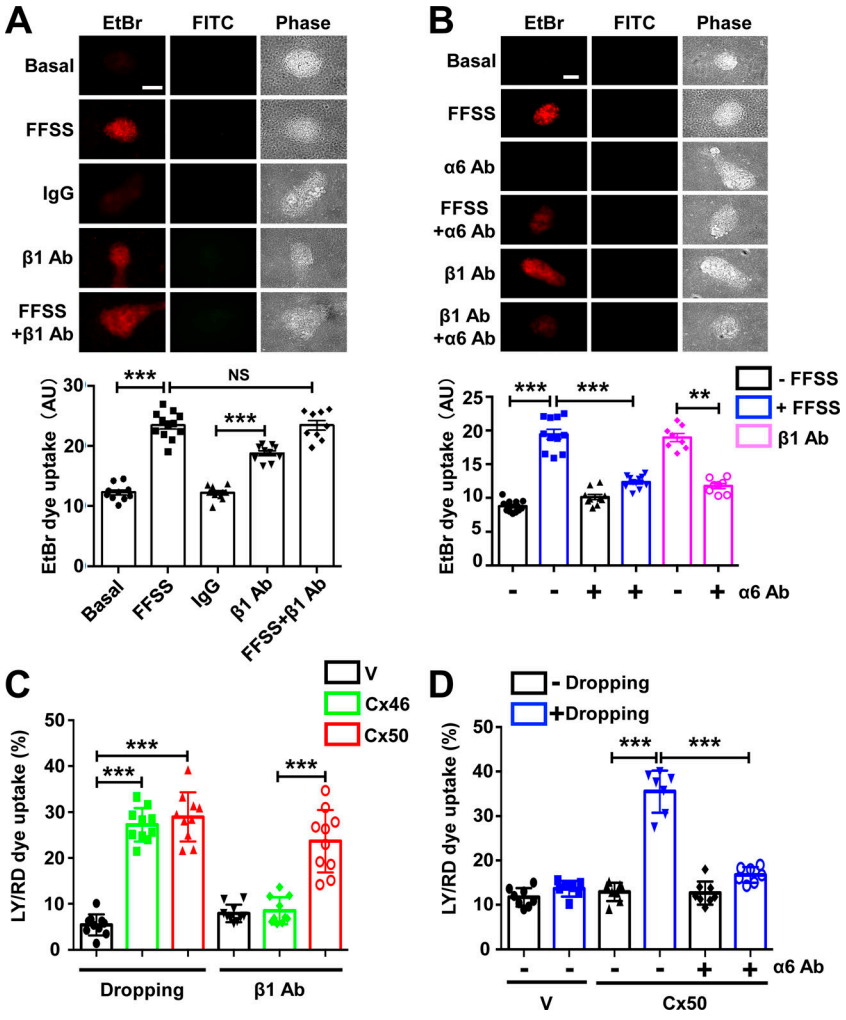

Figure 3. **Hemichannel opening by FFSS is regulated by integrin α6β1. (A)** Differentiated chick lens primary culture was subjected to FFSS or treated with β1 Ab or IgG control at 20 µg/ml for 1 h separately or in combination, followed by EtBr/FITC-dextran dye uptake assay (upper panel). Scale bar, 100 µm. FITC-dextran (M_r 10 kD) was used as a control for nonspecific membrane permeability. The level of dye uptake was quantified by subtracting FITC-positive from EtBr-positive cells (lower panel). Each data point in the graph represents an individual lentoid in one of three independent experiments. **(B)** Differentiated chick lens primary culture was pretreated with integrin α6 blocking antibody (α6 Ab) at 10 µg/ml for 1 h, and then subjected to FFSS, or was pretreated with β1 Ab at 20 µg/ml for 1 h, followed by EtBr/FITC-dextran dye uptake (upper panel). Scale bar, 100 µm. The level of EtBr dye uptake was quantified by subtracting FITC-dextran–positive from EtBr-positive cells (lower panel). Each data point in the graph represents an individual lentoid in one of three independent experiments. **(C)** CEF cells expressing exogenous Cx50 or Cx46 via recombinant RCAS(A) infection or RCAS(A) vehicle control (V) were mechanically stimulated by dropping the medium from a fixed distance or treated with β1 Ab at 20 µg/ml for 1 h. The percentage of LY dye uptake–positive cells per image was quantified by subtracting both LY- and RD-positive cells (M_r 10 kD). Each data point in the graph represents an individual quantified image in one of three independent experiments. **(D)** CEF cells expressing exogenous Cx50 via recombinant RCAS(A) infection or RCAS(A) vehicle control (V) were mechanically stimulated by dropping the medium from a fixed distance or were pretreated with integrin α6 blocking antibody (α6 Ab) at 10 µg/ml for 1 h. The percentage of LY dye uptake positive cells per image was quantified by subtracting both LY- and RD-positive cells. Each data point in the graph represents an individual quantified image in one of three independent experiments. The data are presented as mean ± SEM. NS, not significant; **, P < 0.01; ***, P < 0.001.

(Fig. 4 B). These results suggest that integrin β1 is involved in the regulation of hemichannels opening in Cx50/Cx46-coinfected CEF cells. We further investigated whether integrin α6 is required in heteromeric hemichannel opening. To achieve this, CEF cells were coinfected with Cx50 and Cx46, and followed by α6 Ab treatment before applying fluid-dropping stimulation. The results suggest that integrin α6 is also required in mechanical stimulation–induced hemichannels opening in Cx50/Cx46-coinfected CEF cells (Fig. S4 B). To conclude, these data indicate that integrin α6β1 is an important component in the hemichannel regulatory mechanism, and Cx50 is the dominant player involved in this mechanism.

Integrin α6 interacts with Cx50 at the cytoplasmic C-terminal domain of Cx50

Because Cx50-composed homomeric or heteromeric hemichannels require integrin α6β1 to open under mechanical loading, we set out to determine if integrin α6β1 interacts with Cx50. Therefore, crude membrane protein extracts were generated from the outer cortical fiber layers of E19 chick lenses (as illustrated in Fig. 5 A, left) and incubated with Cx50-CT antibody (against intracellular C-terminal domain of Cx50) or rabbit IgG as a control. As expected, Cx50 antibody immunoprecipitated integrin α6 (Fig. 5 A, right), suggesting an interaction between integrin α6 and Cx50 in lens cortical fibers. Because FFSS increased Cx50 hemichannel activity, we examined whether FFSS would increase integrin α6 and Cx50 association. CEF cells expressing FLAG-tagged Cx50 were subjected to FFSS, and crude membrane protein extracts were collected for immunoprecipitation. FLAG antibody immunoprecipitated more integrin α6 protein in FFSS-treated CEF cells than non–FFSS-treated controls (Fig. 5 B). We took advantage of two naturally occurring truncated forms of Cx50 present in nuclear fibers to identify the Cx50–integrin α6 interacting domains. We previously reported (Wang et al., 2012) that the intracellular C-terminus of Cx50 is first cleaved by caspase 1 at Asp379 and subsequently by caspase 3 at Glu368 during lens development (Fig. 5 C, right). Unlike WT Cx50, hemichannels formed by truncated Cx50 are not responsive to fluid-dropping stimulation (Wang et al., 2012). The truncated mutants, Cx50 368T and Cx50 379T, were expressed in CEF cells through recombinant retroviral infection. Immunoprecipitation by the antibody directed against the intracellular loop domain of Cx50 resulted in undetectable levels of integrin α6 associated with the truncated forms of Cx50 (Fig. 5 C, left).

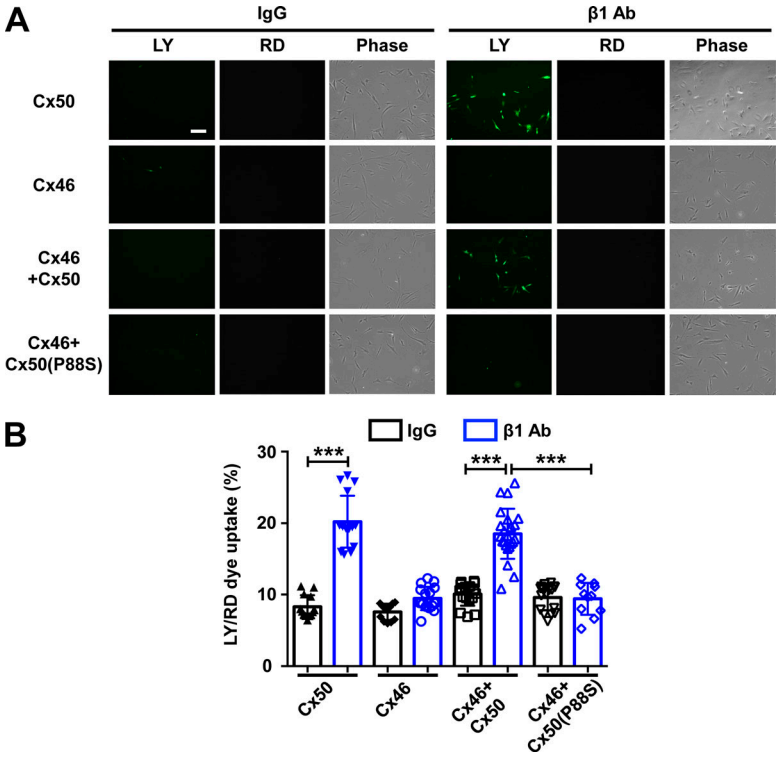

Figure 4. **Activation of integrin β1 opens heteromeric hemichannels formed by Cx50 and Cx46. (A)** CEF cells expressing exogenous Cx46 and Cx50 or Cx50 mutant P88S separately or in combination were seeded at low density to minimize gap junction formation. LY/RD-dextran dye uptake was performed after incubation with control IgG (IgG) or β1 Ab at 20 µg/ml for 1 h. **(B)** The percentage of LY-positive cells per image was counted and quantified by subtracting RD-positive cells. Scale bar, 50 µm. Each data point in the graph represents an individual quantified image in one of three independent experiments. The data are presented as mean ± SEM. ***, P < 0.001.

These results show that the C-terminal domain of Cx50 is involved in the interaction with integrin α6.

Lens hemichannels serve as a transport portal for glucose and GSH

We hypothesized that lens microcirculation, which subjects lens fiber cell membranes to FFSS, opens Cx50 hemichannels. Opened hemichannels allow for the transport of extracellular glucose and antioxidants into cortical lens fibers, and this in turn allows for gap junction delivery of these molecules to mechanically insensitive nuclear fibers. To test this hypothesis, we determined if opened Cx50 hemichannels were permeable to GSH and glucose. GSH and glucose uptake were conducted in differentiated primary chick lens cell cultures. Cx50 dominant-negative mutants were used to determine the involvement of hemichannels in the uptake of GSH and glucose into chick lens cells. Because of the difference in molecular weight, expression of endogenous Cx50 was detected with anti-Cx50 antibody (Fig. 6 A). The GSH uptake assay indicated that FFSS increased GSH uptake in lentoids, while expression of the hemichannel dominant-negative Cx50 mutant (V44A; Shi et al., 2018) significantly reduced the level of GSH uptake in response to FFSS. Like FFSS stimulation, β1 Ab also increased GSH uptake in lentoids (Fig. 6 B). An uptake assay with 2-[*N*-(7-nitrobenz-2-oxa-1,3-diazol-4-yl) amino]-2-deoxy-D-glucose (2-NBDG), a fluorescent glucose analogue, was performed to determine hemichannel glucose permeability in response to FFSS and integrin β1 activation. FFSS increased 2-NBDG uptake in lentoids expressing retroviral vehicle control (V; only endogenous Cx50), exogenous Cx50, or Cx50 mutant (E48K), a Cx50 gap junction dominant-negative mutant. The V44A hemichannel dominant-negative mutant blocked 2-NBDG uptake in response to FFSS, confirming that the glucose (2-NBDG) uptake was dependent on hemichannel opening. Furthermore, integrin β1 activation also increased glucose uptake in lentoids (Fig. 6 C). These results show that activation of hemichannels by FFSS via integrin activation facilitates the transport of glucose and GSH in lens fibers.

We showed that truncated Cx50 was unable to interact with integrin α6. We further tested if hemichannels formed by truncated Cx50 lose their ability to mediate glucose and GSH uptake. CEF cells exogenously expressing Cx50 WT, Cx50 368T, and Cx50 379T were used (Fig. 7 A). Parental CEF cells infected with RCAS(A) retrovirus vehicle were used as a negative control. As expected, FFSS increased GSH uptake in WT Cx50-expressing cells. Treatment with α6 Ab or expression of Cx50 truncation mutants (368T and 379T) significantly decreased Cx50 hemichannel permeability to GSH (Fig. 7 B). Similarly, the level of glucose uptake was analyzed by using 2-NBDG, a fluorescent D-glucose analogue, combined with FACS analysis. FACS analysis showed that FFSS increased 2-NBDG uptake by Cx50 hemichannels, indicated by a rightward peak shift signifying higher 2-NBDG fluorescence intensity (Fig. 7 C, left). Cells treated with α6 Ab or expressing Cx50 truncated mutants failed to show a similar peak shift in response to FFSS. The quantification of mean fluorescent intensity of 2-NBDG based on FACS data confirmed our analytical observations (Fig. 7 C, right).

Active hemichannels are present in isolated, single, short and medium-length cortical lens fiber cells, but not in long nuclear fiber cells

To confirm the location of hemichannels that are responsive to mechanical stress in the lens, we isolated single fiber cells of various lengths. Lens fiber length is indicative of its locations, as fiber length increases from short peripheral cortical fibers to

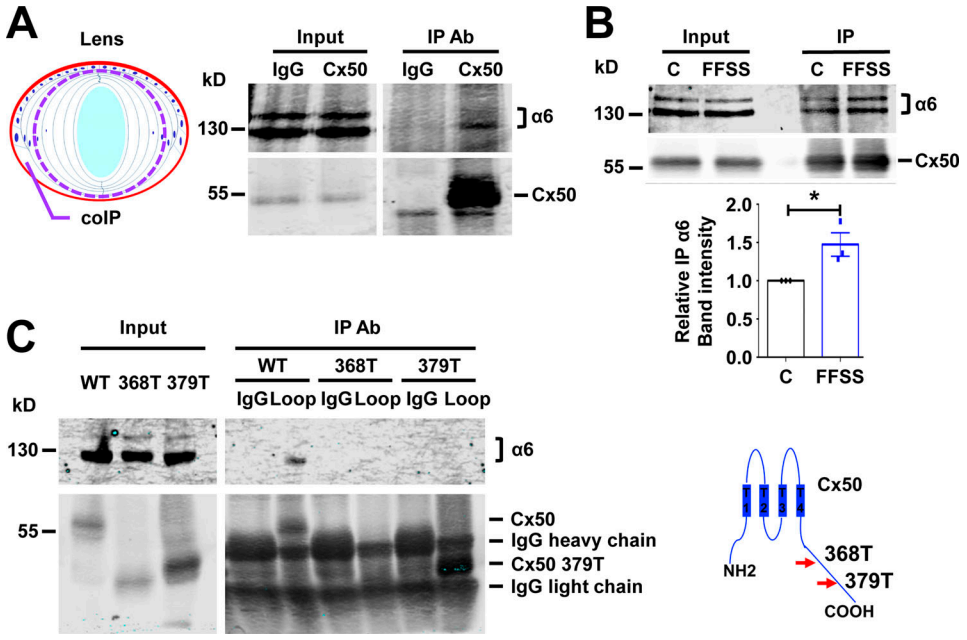

Figure 5. **Integrin α6 associates with lens Cx50. (A)** Crude membrane extracts of cortical fiber portions of E19 chick lens as illustrated in the diagram (left) were collected and immunoprecipitated with control IgG or anti-Cx50 CT antibody. Preloading lysate (Input) and immunoprecipitates (IP) were immunoblotted with anti-integrin α6 and anti-Cx50 loop domain antibody (right). **(B)** CEF cells infected with RCAS(A) Cx50 were subjected to FFSS at 1 dyn/cm^2 for 30 min (FFSS) or under static conditions (C) and immunoprecipitated with anti-FLAG antibody. The immunoprecipitates were immunoblotted with anti-integrin α6 and anti-Cx50 CT antibody (upper panel). Relative immunoprecipitated integrin α6 to immunoprecipitated Cx50 band intensity was quantified (lower panel). Each data point in the graph represents an individual experiment out of three repeats (n = 3). **(C)** CEF cells infected with RCAS(A) Cx50 and Cx50 mutants 368T and 379T. Crude cell membrane extracts were immunoprecipitated with IgG control or anti-Cx50 intracellular loop domain antibody. The immunoprecipitates were immunoblotted with anti-integrin α6 or anti-Cx50 loop domain antibody (left). The truncation sites at C-terminus of Cx50 are indicated (right). Data are presented as mean ± SEM. *, P < 0.05.

long central nuclear fibers. Mechanical stimulation of isolated mouse single fiber cells was achieved by applying spinning force (SF). FFSS or mechanical dropping was not feasible, as these isolated fiber cells do not adhere to cell culture plates. The isolated single fiber cells were mechanically loaded with SF through centrifugation, and an EtBr/FITC-dextran dye uptake assay was conducted. Isolated single fibers from mouse lenses were grouped based on length. We observed that the short and medium-length fibers took up more dye under mechanical stimulation, suggesting that hemichannels on these fibers were responsive to mechanical stimulation. Minimal dye uptake was observed in long fibers under the identical SF applied to short and medium-length fibers (Fig. 8 A). Immunostaining of the isolated lens fibers in suspension with α6 Ab showed lower signals in long fibers than in shorter fiber cells (Fig. 8 B). These results show that reduced or lack of integrin α6 in long fibers, which represent central nuclear fibers, along with Cx50 truncation, may contribute to the unresponsiveness of hemichannels to mechanical stimulation. To further evaluate the contribution of Cx50 hemichannels in the lens, we isolated single lens fiber cells from Cx50 and Cx46 KO mice. Dye uptake in single fiber cells from Cx46 KO and Cx50 KO mice without mechanical stimulation were comparable to those from WT mice, with just a slight reduction in Cx50 KO (Fig. 8 C). Mechanical loading significantly induced dye uptake in both WT and KO models. Cx50 KO significantly decreased SF-induced dye uptake compared with WT fibers. However, Cx46 KO did not show any significant decrease of SF-induced dye uptake compared with WT fibers. Moreover, α6 Ab significantly blocked dye uptake induced by SF only in single cortical fiber cells from WT and Cx46 KO, but not those from Cx50 KO. These results suggest that both monomeric Cx50 and Cx46 hemichannels were responsive to mechanical loading, but only hemichannels containing Cx50 can be regulated by integrin α6. To further demonstrate the important physiological role of Cx50 in modulating oxidative stress level in the lens, we also measured oxidative stress level in the Cx50 KO mouse model. The results showed increased expression of 4-hydroxynonenal (4-HNE) and superoxide dismutase 1 (SOD1) in the cortical lens of Cx50 KO mice compared WT. These data indicate elevated levels of oxidative stress in the Cx50 KO mouse lens and further support our hypothesis that Cx50 hemichannels play an important physiological role in modulating oxidative stress level in the lens (Fig. S5).

Discussion

The delivery of glucose and antioxidants into lens fiber cells is vital to maintain metabolic homeostasis and lens transparency (Braakhuis et al., 2019). As illustrated in Fig. 9 A, we report in this study that lens fiber connexin hemichannels activated by mechanical loading serve as a transport portal for glucose and GSH. Furthermore, integrin α6β1 plays a vital role in the opening of Cx50 hemichannels in response to FFSS, through its interaction with the Cx50 C-terminus. The significance of these findings includes the following. (1) We show that the opening of

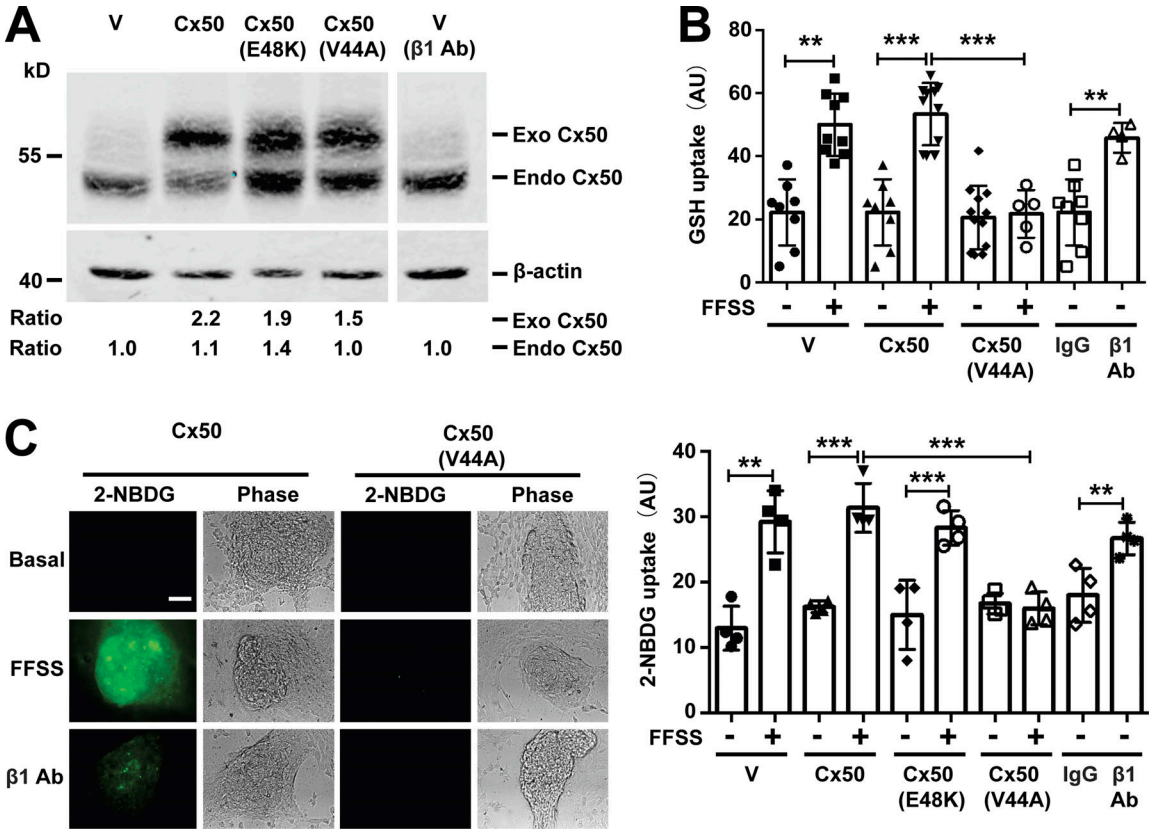

Figure 6. **Hemichannels opened by mechanical loading are permeable to glucose and GSH. (A)** Crude membrane extracts from differentiated chick lens primary culture expressing Cx50 WT or mutants, E48K and V44A were immunoblotted with anti-Cx50 loop domain antibody and β-actin antibody. The expression of Cx50 in the lentoids were quantified. The relative ratio of band intensity of exogenous (Exo) or endogenous (Endo) Cx50 to β-actin with the ratio of the control setting as 1 is shown underneath the immunoblot as indicated. **(B)** Differentiated chick lens primary culture expressing Cx50 WT or mutant, V44A, was subjected to FFSS for 30 min or was treated with control IgG or β1 Ab at 20 µg/ml for 1 h, and GSH uptake was performed and quantified. Each data point in the graph represents an individual lentoid in one of three independent experiments. **(C)** Differentiated chick lens primary culture expressing Cx50 WT or mutants, E48K and V44A, was subjected to FFSS for 30 min or was treated with control IgG or β1 Ab at 20 µg/ml for 1 h before 2-NBDG uptake assay (left). Bar, 50 µm. The level of 2-NBDG uptake in lentoids was quantified (right). Each data point in the graph represents an individual lentoid in one of three independent experiments. All data are presented as mean ± SEM. **, P < 0.01; ***, P < 0.001.

Cx50 hemichannels by mechanical stimulation contributes to the transport of GSH and glucose in the lens, an important process for maintaining lens hemostasis and transparency. It has been proposed that the lens may use a unique internal microcirculation system to deliver antioxidants and nutrients to different regions of lens fibers; however, the specific delivery mechanism remained unclear (Braakhuis et al., 2019; Donaldson et al., 2001). The results in this study propose a new mechanism by which Cx50 hemichannels facilitate GSH and glucose transport into lens cortical fibers, and this process is driven by FFSS, likely generated by lens internal microcirculation. (2) This study reports a new mechanotransduction mechanism in which the opening of Cx50 hemichannels under mechanical stimulation is dependent on integrin α6β1 function and interaction. We demonstrate the interaction between Cx50 and integrin α6 and identify an integrative domain in Cx50. Moreover, nuclear lens fibers lose the responsiveness of Cx50 hemichannels to mechanical stimulation upon natural truncation of this domain. (3) With the successful isolation of single lens fiber cells in WT and connexin KO mouse models, we were able to define the hemichannel and integrin function at different lens regions in response to mechanical stimulation.

Because of the lack of vasculature, long-lasting, vulnerable lens fiber cells rely heavily on extracellular glucose, GSH, and other molecules to maintain their hemostasis and transparency, as illustrated in Fig. 9 B. The lens maintains very high concentrations (~3–5 mM) of the antioxidant GSH (Whitson et al., 2016). A GSH concentration gradient exists within the lens, with the highest levels in the outer cortical fibers gradually decreasing toward the central nuclear fibers (Donaldson et al., 2010; Srinivas, 2014). However, it is unclear that the total amount measured represents GSH inside the cell or in the extracellular fluid. The source of GSH is believed to be endogenous (synthesized by epithelium and immature lens fiber) and exogenous (vitreous humor and aqueous humor; Whitson et al., 2016). Our model depicts that extracellular GSH, released by either lens epithelium/immature lens fibers or vitreous/aqueous humor, is taken up by connexin hemichannels in cortical fibers. Because connexin truncation renders hemichannels unresponsive to FFSS, GSH in cortical fibers is delivered to inner core nuclear fibers through gap junction channels (Slavi et al., 2014). Therefore, hemichannels activated in outer cortical fibers by mechanical stress assist in the transport of GSH into central,

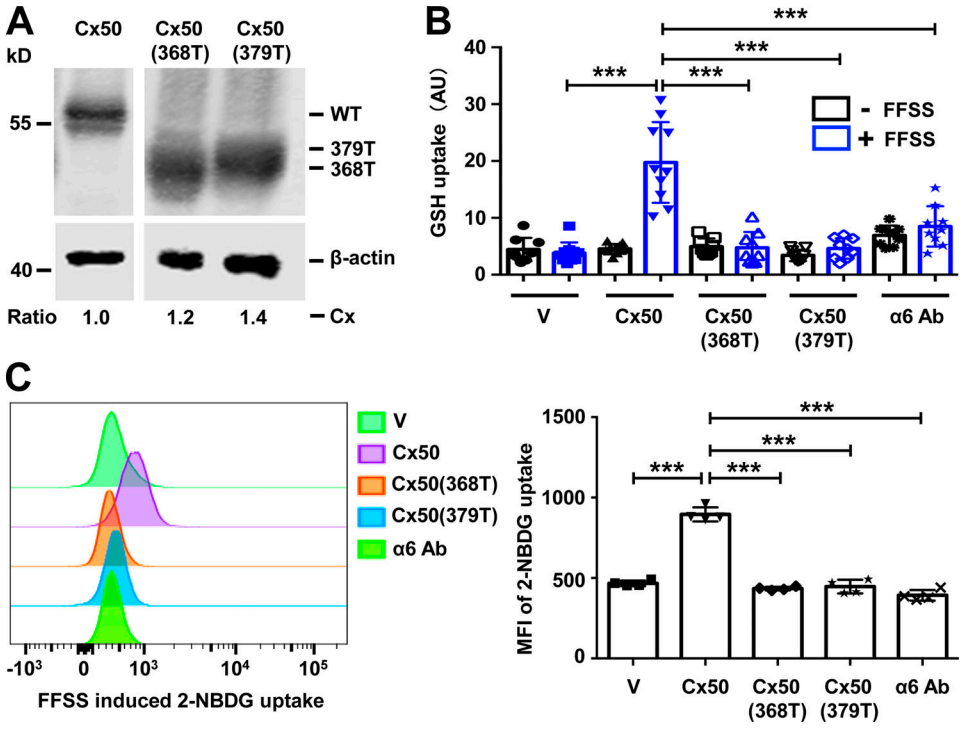

Figure 7. **Association of integrin α6 and Cx50 is essential for the permeability of glucose and GSH through hemichannels. (A)** Crude membrane extracts from CEF cells infected with RCAS(A) vehicle (V), Cx50 WT, or Cx50 truncation mutants 368T or 379T were isolated and immunoblotted with anti-Cx50 loop antibody anti-β-actin antibody. The expression of retrovirus-induced exogenous connexins in the CEF cells was quantified. The relative ratio of band intensity of Cx50 or truncated mutants to β-actin with the ratio of the control setting as 1 is shown underneath the immunoblot. **(B)** CEF cells were infected with RCAS(A) containing Cx50 WT, Cx50(368T), Cx50(379T), or RCAS(A) vehicle control (V). Cx50 WT was pretreated with or without α6 blocking antibody at 10 µg/ml for 1 h, and then subjected to FFSS for 30 min or under static conditions. GSH uptake was conducted and quantified. Each data point in the graph represents an individual quantified image in one of three independent experiments. **(C)** CEF cells were infected with RCAS(A) containing Cx50 WT or mutants 368T and 379T, or RCAS(A) vehicle control (V). WT Cx50 was pretreated with or without anti-integrin α6 antibody at 10 µg/ml in glucose free medium for 1 h. Cells were then subjected to FFSS for 30 min or under static conditions. Glucose uptake was conducted and analyzed by flow cytometry (left). The mean fluorescent intensity of 2-NBDG uptake was quantified (right). Each data point in the graph represents an individual quantified image in one of three independent experiments. All data are presented as mean ± SEM. ***, P < 0.001.

nuclear fibers. In addition to GSH, in one study the mean plasma and aqueous glucose levels were reported as 5.8 and 3.2 mM, respectively (Davies et al., 1984). Another study showed glucose concentrations in anterior aqueous humor of 137 mg/100 ml (7.6 mM), and it was speculated that glucose concentration was ∼100 mg/100 ml (5.5 mM) in extracellular lens fluid (Kuck, 1965). Glucose in the lens cell is primarily from aqueous humor (Swarup et al., 2018), and glucose is converted into glucose-6-phosphate rapidly inside cells (Kinoshita, 1965). Although the gradient of glucose from the cortex to the nucleus has not been directly measured, we would expect that glucose in the microfluidic solution is higher than that inside the lens cells, and like GSH, there is a gradient, with the highest level of glucose found in cortical fibers. We found that Cx50 hemichannels are permeable to glucose and GSH in response to FFSS. In addition, our data show that Cx50 deficiency in the KO mouse model leads to increased oxidative stress compared with WT control mice. These findings support the physiological role of Cx50 hemichannels in reducing oxidative stress by mediating the transport of antioxidants. An unresolved question is how the normally robust oxygen radical scavenger system fails with aging. Increased oxidative stress is a major concern, since it is associated with increased protein aggregation and lens opacities, specifically in the lens nucleus (Braakhuis et al., 2019). This might be explained partially by our study that truncated Cx50, which accumulates in nuclear fiber cells in aged lens (Wang et al., 2012; Yin et al., 2001), leads to decreased delivery of GSH, glucose, and other metabolites to the lens nuclear fibers owing to mechano-unresponsive hemichannels.

Integrins, known as mechanical sensory molecules, are reported in vascular endothelial cells and bone cells (Batra et al., 2012; Katsumi et al., 2004; Sun et al., 2016). There is a high degree of colocalization between Cx50 and integrin α6 in nascent lens fibers and the apical side of lens epithelial cells. In addition to β1, α6 can be a partner with integrin β4. A previous study shows that in differentiating lens fiber cells, α6β4 is localized to the basolateral tips of the cells, while α6β1 localizes along cell–cell interfaces (Walker and Menko, 2009). We showed that blocking α6 integrin activation almost completely ablated the effect of β1 Ab on the opening of hemichannels, suggesting the functional partnership of α6β1 heterodimers in activation of hemichannels. We believe that α6β4, although it is expressed in the lens, is unlikely to be involved in the activation of hemichannels. Because of the extracellular spaces between lens

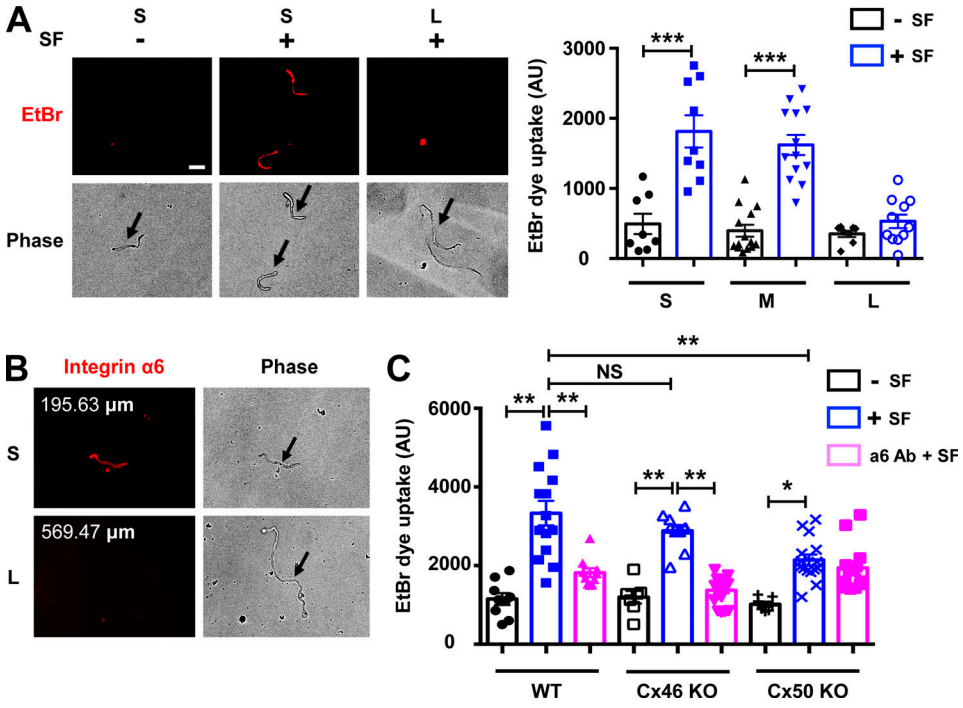

Figure 8. **Integrin α6 is required for Cx50 hemichannel opening. (A)** Different lengths of single lens fiber cells were isolated from WT mice and mechanically loaded by spinning force (SF; 1,000 rpm for 5 min). An EtBr dye uptake assay was performed. Scale bar, 50 μm (left). The morphology of unhealthy fiber cells resembles resealed globules or has a rounded appearance (Bhatnagar et al., 1995). Unhealthy or dead fibers are readily distinguished by their morphology without using FITC dextran. Isolated single fibers were grouped by their lengths; short fibers (S) were <200 μm long; medium fibers (M) were 200 to 400 μm; and long fibers (L) were >400 μm. EtBr dye uptake intensity was quantified by ImageJ (right). **(B)** Isolated single lens fibers were obtained from WT mouse lenses and immunostained with integrin α6 antibody. **(C)** Single lens fibers were isolated from WT, Cx46 KO, and Cx50 KO mouse lenses. The fibers were pretreated with or without anti-integrin α6 antibody (α6 Ab; 10 μg/ml for 20 min), and EtBr dye uptake assay was performed during mechanical stimulation with SF (1,000 rpm for 5 min). EtBr dye uptake intensity in short fibers was quantified. Each data point in the graph represents an individual single fiber in one of three independent experiments. All data are presented as mean ± SEM. NS, not significant; *, P < 0.05; **, P < 0.01; ***, P < 0.001.

epithelial cells and underneath lens fibers and between fiber cells, FFSS is expected to be generated there and sensed by integrins. We show here that activation of integrin α6β1 in lens cortical fiber cells under mechanical stimulation activates Cx50 hemichannels. Given the colocalization of integrin α6β1 and Cx50 in lens epithelial cells, we conducted studies in lens epithelial cells similar to those in the differentiated lens fiber cells. Our results point to a similar mechanoactivation mechanism for hemichannels in lens epithelial cells. After a brief mechanical stimulation, the increased interaction between integrin α6 and Cx50 is possibly caused by the increased trafficking of integrin to the membrane. The presence of α6 along the long cell–cell borders of nascent fiber cells, in the absence of any known extracellular matrix ligands (Walker and Menko, 2009), leads us to postulate that integrin α6β1 mediates Cx50 hemichannel opening in a ligand-independent manner.

Cx50 and Cx46 in lens fibers form heteromeric hemichannels (connexons; Jiang and Goodenough, 1996). There might be coexistence of three types of hemichannels in lens fibers: hemichannels formed by Cx50, Cx46, and both Cx50 and Cx46. To date, because of technical challenges, there is no reported study elucidating the presence and distribution of these types of hemichannels. Dominant-negative mutant P88S completely impairs Cx46 hemichannel function, indicating that heteromeric hemichannels are primarily present when Cx50 and Cx46 are coexpressed. Furthermore, integrin β1 activation induces the opening of hemichannels in cells expressing Cx50 or coexpressing Cx50 and Cx46, but not in cells expressing only Cx46; this provides evidence for functional heteromeric hemichannel formation. These results suggest that Cx50 is required in the regulation of heteromeric hemichannels by integrin α6β1 in response to mechanical stimulation.

During lens development, young cells continually arise in the equator and outer cortex layers. The majority of the cells in the central core region are fully differentiated lens nuclear fibers. The length of the cortical fiber cells defines their physical location within the lens; short young fiber cells are located in the equator region, followed by medium-length cells, and then the long fiber cells near the central nuclear fiber region (Gangalum et al., 2018). Freshly isolated short and medium-length fiber cells are responsive to mechanical stimulation, unlike freshly isolated long fibers. We reason that the absence of integrin α6 in long fibers, representing the central nuclear lens fiber region, may explain the lack of a mechanical response. Similar to WT, fiber cells isolated from Cx46 KO mice showed a consistent responsiveness to mechanical stimulation and a similar dependence on α6 integrin activation. These data confirm that integrin α6β1 plays an essential role in opening hemichannels, and that Cx50 is the connexin involved in this mechanism. Because Cx46 is also responsive to mechanical stimulation, Cx50 KO, as expected, still showed a reduced level of hemichannel activity because of

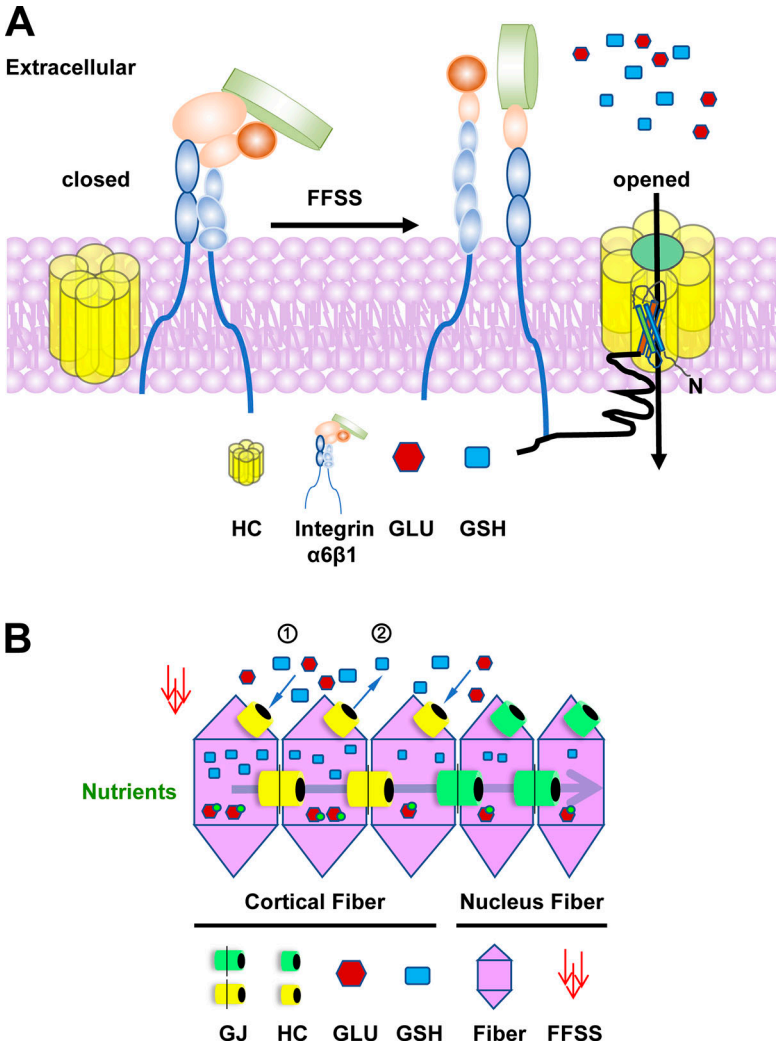

Figure 9. **Diagram of the mechanism of connexin hemichannels activated by FFSS and the mechanism of glucose and GSH transport to achieve lens fiber homeostasis. (A)** FFSS induced by flow of fluid in the microcirculation leads to conformational activation of integrin α6β1. Activated integrin α6β1 enhances the association with C-terminus of Cx50 (black tail) and facilitates connexin hemichannels opening and the transport of GLU and GSH into lens fiber cells. **(B)** Cx50 hemichannels act as a transport portal for the uptake of GLU and GSH into the outer cortical fibers when glucose and GSH concentrations in the extracellular space are higher than those of the intracellular space (1). Cx50 hemichannels could also release GSH by outer lens epithelium/immature fibers when GSH concentration is higher intracellularly than extracellularly (2). This process helps GSH diffuse to proximal lens fiber cells. Glucose might not be able to release from fiber cells because glucose turns to glucose-6-phosphate rapidly inside cells (Kinoshita, 1965). Because of the physiological barrier (Michael and Bron, 2011), nutrients and antioxidants taking up from outer cortical fibers will be transported from outer lens to the nuclear fibers through gap junctions, likely by Cx46 (Slavi et al., 2014). In the nuclear fibers, because of the absence of integrin α6β1 and truncation of Cx50 at its C-terminus, hemichannels formed by truncated Cx50 (green) are not responsive to mechanical stimulation and thus remain closed. In this diagram: HC, hemichannel; yellow, full-length HC; green, truncated HC; GJ, gap junction; GLU (red hexagon), glucose; red hexagon with green dots, glucose-6-phosphate.

the presence of Cx46, which is consistent with what we observed in cultured cells. However, in the Cx50 KO, the increased hemichannel activity in response to mechanical stimulation was not inhibited by α6 Ab. This confirms the regulatory role of the integrins on Cx50. Therefore, a similar mechanism is demonstrated in single lens fiber cells and in cell models. Of course, we cannot exclude the possibility of a compensatory effect by Cx50 or Cx46, respectively, or up-regulation of other mechanisms in the KO models. The molecular mechanism for Cx46 hemichannel activation under mechanical stimulation remains unknown, but could involve interaction with other mechanical sensors, or possibly direct activation by mechanical loading.

Taken together, these data show that activation of connexin hemichannels in outer cortical lens fibers through mechanical activation of integrins likely plays a critical role in glucose and GSH transport. This hemichannel response to mechanical stimulation functions in maintaining metabolic homeostasis and lens transparency. Elucidating the mechanistic roles of connexin hemichannels in the lens will provide insights into the function of these channels in hemichannel-rich tissues, such as brain and bone, under physiological and pathological conditions.

Materials and methods

Materials

Fertilized white leghorn chicken eggs were obtained from Texas A&M University Agriculture & Poultry Science. Rabbit anti-FLAG monoclonal antibody was obtained from Rockland (600-401-383), and rabbit anti-Cx50 was generated and affinity-purified as previously reported (Jiang et al., 1994). Rat integrin α6 functional blocking antibody (10 μg/ml) was obtained from R&D Systems (MAB13501; Primo et al., 2010). Mouse anti-chicken integrin α6 for Western blot was obtained from the Developmental Studies Hybridoma Bank (P2C62C4; Walker et al., 2002). Mouse β1 Ab was obtained from Santa Cruz Biotechnology (SC53711). PFA (16% stock solution) was obtained from Electron Microscope Sciences. FBS was obtained from Hyclone Laboratories. Protein A/G plus agarose was obtained from Santa Cruz Biotechnology (sc-2003). Type 1A collagenase was obtained from Sigma-Aldrich. Rabbit anti-4-HNE antibody was obtained from Abcam (ab46545), and rabbit anti-SOD1 antibody was obtained from Santa Cruz Biotechnology (SC11407). All other chemicals were obtained from either Sigma-Aldrich or Thermo Fisher Scientific.

Preparation of retroviral recombinant DNA constructs and high-titer retroviruses containing Cx50 truncation mutants

Retroviral constructs and high-titer retroviruses were prepared based on our previously described protocol (Jiang, 2001; Jiang and Goodenough, 1998). Briefly, a DNA fragment containing wild-type Cx50 with a FLAG tag linked at the Cx50 C-terminus was made by PCR and constructed into the retroviral vector RCAS(A). We have shown that, compared with untagged connexin, the FLAG tag has a minimal effect on membrane distribution and activities of connexin channels (Jiang and Goodenough, 1998). With the wild-type RCAS(A)-Cx50 DNA construct as a template, retroviral constructs of Cx50 truncation mutants were generated with the following pairs of primers: Cx50(368T): sense, 5′-GACTACAAGGACGACGATGAC-3′, and antisense, 5′-CACTTCATCGCTCACCACCT-3′; Cx50 (379T): sense, 5′-GACTAC AAGGACGACGATGAC-3′, and antisense 5′-ATCGGTGGCAAG TTCAGCAG-3′.

High-titer recombinant retroviruses were generated (1×10^8 to 5×10^8 CFU/ml) through transfection of these DNA constructs into CEF cells using Lipofectamine according to the manufacturer's instructions (Thermo Fisher Scientific). Conditioned media were collected and concentrated to generate high-titer recombinant retrovirus.

Cell culture and retroviral expression

Two cell culture models were used in this study: chick embryonic fibroblast (CEF) cells and primary chick lens cells that can differentiate into lens fiber-like "lentoid" structures. CEF cells were cultured in DMEM plus 10% FCS and 2% chick serum. CEF cells were infected with high-titer retroviruses on the second day of culture. After reaching confluence, CEF cells were digested with 0.05% trypsin and passaged. Primary chick lens cell cultures were prepared by a modified method as described previously (Jiang et al., 1993; Menko et al., 1984). For primary chick lens cell cultures, lenses from 11-d-old chick embryos were dissected, washed with TD buffer (140 mM NaCl, 5 mM KCl, 0.7 mM Na_2HPO_4, 5 mM glucose, and 25 mM Tris-HCl, pH 7.4), digested with 0.1% trypsin in TD buffer at 37°C for 30 min, and homogenized in M199 medium plus 10% FBS. Cells were washed and resuspended in M199 medium. Living cells were then counted and seeded at 2×10^6 cells per 60-mm collagen-coated cell culture dish. On the second day of cell culture, high-titer recombinant retroviruses containing Cx50 WT or mutants were added to primary lens cell cultures. The cultures were incubated at 37°C with 5% CO_2 and fed every 2 d. In the beginning of culture, monolayer lens epithelial cells, but not fiber cells, proliferated on the culture plates. After 4–5 d, lens epithelial cells became confluent and began to differentiate and form lentoids. We followed the Animal Research: Reporting of In Vivo Experiments guideline to ensure proper reporting of in vivo experiments. The protocol of using chicken embryos was reviewed and approved by our Institutional Animal Care and Use Committee.

Immunohistochemistry

E18 embryo mouse eyeballs were carefully dissected and fixed in 2% PFA (diluted from 16% stock in PBS) for 2 h at room temperature. Eyeballs were immersed in 1 M sucrose overnight at 4°C and then in Tissue-Tek compound for 5 min, before quickly being frozen in Tissue-Tek optimal cutting temperature compound (Sakura Finetek USA) by immersing in liquid nitrogen. Sagittal frozen lens tissue sections (12-µm thickness) were prepared. For dual immunolabeling of integrin α6 and Cx50, frozen lens sections were first incubated in PBS for 5 min to remove optimal cutting temperature compound and then in blocking solution (2% normal donkey serum, 2% fish-skin gelatin, 0.25% Triton X-100, and 1% BSA in PBS) for 1 h at room temperature, followed by incubation with anti-integrin α6 antibody (1:50 dilution; MAB13501; R&D Systems) in blocking solution overnight at 4°C. After proper washing, affinity-purified anti-Cx50 primary antibody (1:5,000 dilution) was applied for 1 h at room temperature. Lens tissue sections were washed four times for 5 min with PBS, and then incubated with rhodamine-conjugated donkey anti-rat secondary antibody (1:500 diluted in blocking solution) for integrin α6 and Alexa Fluor 488-conjugated donkey anti-rabbit secondary antibody (1:500 diluted in blocking solution) for Cx50 for 1 h at room temperature. After washing with PBS four times, tissue sections were preserved in mounting medium. Control experiments were conducted by labeling with primary antibody sequentially to ensure that binding of one antibody was not sterically hindered by the other and labeling with preimmune antibody to determine any nonspecific binding. The specimens were mounted with Vectashield, examined with a Zeiss LSM 710 confocal microscope with 63× NA 1.40 oil differential interference contrast objective at room temperature (22°C) using Zeiss Zen 2011 software. The images were processed using Photoshop and ImageJ (1.50i; National Institutes of Health) by cropping and converting to RGB, generating maximum-intensity projections, and adding scale bars. The colocalization coefficiency between integrin α6 and Cx50 was quantified with ImageJ.

Immunostaining of integrin α6 on the isolated single mouse lens fiber was conducted in cell suspension. Briefly, collected individual fiber cells were fixed in 2% PFA for 30 min at room temperature, followed by incubation in blocking solution (2% normal donkey serum, 2% fish-skin gelatin, 0.25% Triton X-100, and 1% BSA in PBS) for 1 h at room temperature, and then incubated with anti-integrin α6 antibody (MAB13501; 1:50 dilution; R&D Systems) in blocking solution at 4°C overnight. After proper washing, rhodamine-conjugated donkey anti-rat secondary antibody (1:500 dilution) was applied for 1 h at room temperature. In each washing step, fibers were collected by centrifuging at 200 *g* for 5 min.

Preparation of cell membrane extracts and Western blotting

Confluent cultured CEF cells or cultured differentiated primary chick lens cells were collected in lysis buffer (5 mM Tris, 5 mM EDTA, and 5 mM EGTA, pH 8.0) plus protease inhibitors (phenylmethylsulfonyl fluoride, *N*-ethylmaleimide, Na_3VO_4, and leupeptin) and ruptured by triturating through a 26.5-gauge needle 20 times. Crude membranes were pelleted by centrifugation at 124,000 *g* for 45 min (TLA55 rotor; Beckman Coulter) at 4°C. Pellets were resuspended in lysis buffer and boiled in 0.6% SDS. MicroBCA assay (Pierce) was used to quantify protein concentration. 20 µg sample per lane was loaded on a 10% SDS-PAGE

gel and then electrotransferred onto a nitrocellulose membrane. The membrane was immunoblotted with primary antibodies, and primary antibodies were detected with goat anti-rabbit IgG conjugated IRDye 800CW or goat anti-mouse IgG conjugated IRDye 680RD (1:15,000 dilution) using a Licor Odyssey Infrared Imager. The intensity of the bands on Western blots was quantified with ImageJ.

FFSS, fluid dropping, and mechanical loading by spinning force

Three methods, FFSS, fluid dropping, and spinning force, were used to apply mechanical stimulation accordingly to primary chick lens cell culture, CEF cells, and isolated single mouse lens fibers. FFSS and fluid dropping experiments were conducted to apply mechanical stress to adherent cultured cells as described previously (Burra et al., 2010; Cheng et al., 2001; Riquelme et al., 2015). Briefly, fluid flow was generated by parallel plate flow chambers separated by a gasket of defined thickness with gravity-driven fluid flow using a peristaltic pump. The shear stress level was determined by channel height and gasket thickness. Stress level of 1 dyn/cm^2 was generated and applied. Primary chick lens cell culture was seeded on a collagen-coated glass slide and put in the parallel chamber during FFSS stimulation. CEF cells were seeded 24 h before fluid-dropping experiments in a 35-mm^2 cell culture dish at a low cell density to ensure that the majority of the cells were not in physical contact (minimizing formation of gap junctions). Fluid dropping was conducted by dropping 200 µl of α-MEM from a fixed distance as previously reported (Burra et al., 2010). Unlike cultured cells, isolated mouse lens fibers are not attached to the culture plates; therefore, it is not feasible to use FFSS or fluid dropping to introduce mechanical stimulation. Therefore, we used spinning force to apply mechanical stimulation to nonadherent single fiber cells. Briefly, freshly isolated single mouse lens fibers were suspended in artificial aqueous humor (AAH buffer: 149 mM NaCl, 4.7 mM KCl, 2.5 mM $CaCl_2$, 5 mM glucose, and 5 mM Hepes, pH 7.4). Mechanical loading was applied by centrifuging fibers at 160 *g* for 5 min in the presence of 0.1 mM EtBr. Nonloaded fibers in 0.1 mM EtBr for 5 min served as a control. Dye uptake was quantified using ImageJ. Arbitrary units (AU) given by ImageJ are reflective of fluorescence intensity. The mean fluorescence intensity is presented, quantified as total fluorescence intensity divided by stained area.

Coimmunoprecipitation assay

For immunoprecipitation experiments, cortical fiber portions of embryonic day 19 chick lenses were collected. CEF cells were coinfected with recombinant retroviruses containing WT Cx50 and Cx50 truncation mutants: Cx50(368T) and Cx50(379T). Crude membranes were prepared similarly as described above (Western blotting), while the pellets were resuspended in immunoprecipitation buffer (100 mM NaCl, 15 mM EDTA, 20 mM $Na_2B_4O_7$, and 0.5% Triton X-100, pH 8.5) for coimmunoprecipitation assays. Lysates (120 µg per sample) were precleared with protein A/G plus agarose beads (sc2003; Santa Cruz) and pelleted by centrifugation at 1,000 *g* at 4°C for 5 min. Supernatants (precleared lysates) were then incubated with anti-Cx50 CT, anti-Cx50 Loop (against intracellular loop domain of Cx50), anti-FLAG tag, or rabbit IgG antibody at 4°C overnight, followed by precipitation of the complexes after incubation with 120 µl of protein A/G plus agarose beads for 2 h at room temperature. Immunoprecipitates were collected in reducing or nonreducing sample buffer for detection of integrin α6 or Cx50, respectively, separated on 10% SDS-PAGE gels, and immunoblotted with anti-Cx50 antibody or anti-integrin α6 antibody, respectively.

Hemichannel dye uptake assay

Primary chick lens cell culture and CEF cells were infected with RCAS(A) vehicle control or recombinant RCAS(A) containing Cx50, Cx46, Cx50 site, or truncated mutants. Primary lens cells were cultured until lens epithelial cells differentiated into lentoid structures. EtBr (M_r ~394 D) was used in primary lens cell culture as a tracer to detect hemichannel activity, and FITC-dextran (M_r ~10 kD), which is too large to pass through hemichannels but is taken up by dying cells, was used as a control. Dye uptake experiments were conducted in the presence of 0.1 mM EtBr and 1 mg/ml FITC-dextran for 5 min, and the cells were rinsed three times with HBSS and fixed with 2% PFA for 30 min. We quantified the mean fluorescence intensity of the lentoids in the differentiated primary chick lens cell cultures using ImageJ.

CEF cells were exposed to a 0.4% LY (M_r ~457 D) and 0.4% rhodamine dextran (RD; M_r ~10 kD) dye mixture in the fluid-dropping medium during fluid dropping for 5 min, followed by three washes with HBSS and fixation with 2% PFA for 30 min. RD fluorescence cells were excluded as nonspecific permeable, dying cells. The percentage of LY fluorescent cells (excluding LY and RD double-positive cells) to total cells per image was calculated and plotted. Freshly isolated single mouse lens fibers were exposed to 0.1 mM EtBr in AAH buffer for 5 min, followed by three washes with AAH buffer and fixation with 2% PFA for 30 min. Mean fluorescence intensity in the lens fibers was quantified using ImageJ.

GSH and glucose transport assay

GSH and glucose transport assays were performed in the differentiated primary lens culture containing lentoids and CEF cells. We cultured primary chick lens cells on a collagen-coated glass in a 60-mm culture dish until lentoids formed. For CEF cells, subconfluent cells were seeded at 10^6 cells/well on collagen-coated glass in a 60-mm culture plate 24 h before the experiments. We determined GSH transport by performing uptake measurement with ThiolTracker (Thermo Fisher Scientific). Briefly, after being subjected to FFSS at 1 dyn/cm^2 for 30 min, cells were preincubated with 1 mM GSH for 30 min. Cells were then rinsed with HBSS and incubated with 10 µM ThiolTracker for 5 min at room temperature. Cells were rinsed three times with PBS and fixed with 2% PFA. The conjugation of ThiolTracker and GSH formed a fluorescent molecule, and fluorescence intensity was measured and quantified using ImageJ.

A fluorescent D-glucose analogue, 2-NBDG (NC0292035; Thermo Fisher Scientific) was used to measure glucose uptake. All cultured cells were starved in glucose-free medium (PBS plus 10% BSA) for 1.5 h. The cells were then subjected to FFSS at 1 dyn/cm^2 for 30 min and exposed to glucose-free medium

containing 300 µM fluorescent 2-NBDG (Zou et al., 2005) for 20 min at room temperature. 2-NBDG uptake was terminated by removing the medium and washing the cells twice with cold PBS. For primary lens culture, cells were fixed with 2% PFA for 30 min and imaged. CEF cells were trypsinized and subsequently resuspended in 200 µl of 1% PFA plus 2% FBS in PBS at room temperature for 30 min before flow cytometry analysis. For each measurement, data from >2,000 single-cell events were collected using a FACS Celesta flow cytometer (BD Immunocytometry Systems) within 20 s. 2-NBDG fluorescence, sensitive to its microenvironment, typically displays excitation/emission of ∼465/540 nm.

Single fiber cell isolation from mouse lens

The process of single lens fiber isolation was performed according to published protocols, with modifications (Ebihara et al., 2011; Webb et al., 2004). Briefly, 1-mo old mice were sacrificed by isopropanol asphyxiation and cervical dislocation. The lenses were dissected free from the extracted eyes and placed in AAH buffer. Adherent nonlens material was carefully removed from the lens. A posterior tear was made on the lens capsule, and the capsule was removed. The capsule and the other bulk of the lens were incubated with dissociation buffer (170 mM Na-gluconate, 4.7 mM KCl, 5 mM Hepes, 5 mM glucose, and 0.125% [wt/vol] type 1A collagenase) at 35°C for 35–40 min, with occasional gentle flicking to reexpose settled cell clumps to the enzyme solution. Cells were gently vortexed before collection by centrifugation at 1,000 rpm for 2 min. Pelleted cells were resuspended in 200 µl AAH consisting of 10% FBS to inactivate collagenase, followed by appropriate washing. Hemichannel activity in single lens fibers induced by mechanical loading (spinning force) was assessed immediately after isolation. All animal-related procedures were approved by the Institutional Animal Care and Use Committee at the University of Texas Health Science Center at San Antonio.

Statistical analysis

All data were analyzed with Prism 6 (GraphPad Software). Two group comparisons were performed using Student's *t* test (unpaired, two sided, and 95% confidence interval). Multiple group comparisons were conducted using one-way ANOVA, followed by Tukey's multiple comparison test. Colocalization analyses were determined by the Mander's correlation coefficient per region of interest using ImageJ. For all analyses, data distribution was assumed to be normal but was not formally tested. The data are presented as mean ± SEM of three independent measurements. A P value <0.05 was considered statistically significant. Asterisks in all figures indicate the degree of significant difference compared with controls: NS, not significant; *, $P < 0.05$; **, $P < 0.01$; and ***, $P < 0.001$.

Online supplemental material

Fig. S1 shows that fluid dropping has mechanical stimulatory effect similar to that of FFSS. Fig. S2 shows that integrin α6 is expressed in cortical lens tissue, primary chick lens culture, and CEF cells. Fig. S3 shows that our proposed hemichannel regulatory mechanism by integrin α6β1 in lens fibers also applies to that in lens epithelial cells. Fig. S4 (related to Fig. 4) shows that integrin α6 is required for heteromeric hemichannel opening. Fig. S5 shows that oxidative stress is increased in Cx50-deficient mouse lens.

Acknowledgments

The authors thank Dr. Thomas White at Stony Brook University for generously providing Cx50 and Cx46 KO mice, Dr. Exing Wang at the Institutional Optical Imaging Facility at UT Health San Antonio for technical help on confocal imaging, Bogang Wu for technical help with flow cytometry analysis, and Dr. Eduardo R. Cardenas for proofreading and editing the manuscript.

The study was supported by National Institutes of Health RO1 EY012085 and Welch Foundation grant AQ-1507 to J.X. Jiang.

The authors declare no competing financial interests.

Author contributions: J. Liu conducted conceptualization, data curation, investigation, methodology, validation, visualization, original draft writing, and review and editing. M.A. Riquelme conducted conceptualization, investigation, methodology, validation, and visualization. Z. Li, Y. Li, Y. Tong, and Y. Quan conducted methodology, investigation, and review and editing. C. Pei conducted supervision and review and editing. S. Gu conducted conceptualization, formal analysis, investigation, methodology, supervision, and review and editing. J.X. Jiang conceived the study and conducted conceptualization, formal analysis, funding acquisition, project administration, resources, supervision, draft writing, and review and editing.

Submitted: 26 February 2020
Revised: 1 September 2020
Accepted: 28 September 2020

References

Banks, E.A., X.S. Yu, Q. Shi, and J.X. Jiang. 2007. Promotion of lens epithelial-fiber differentiation by the C-terminus of connexin 45.6 a role independent of gap junction communication. *J. Cell Sci.* 120:3602–3612. https://doi.org/10.1242/jcs.000935

Batra, N., S. Burra, A.J. Siller-Jackson, S. Gu, X. Xia, G.F. Weber, D. DeSimone, L.F. Bonewald, E.M. Lafer, E. Sprague, et al. 2012. Mechanical stress-activated integrin α5β1 induces opening of connexin 43 hemichannels. *Proc. Natl. Acad. Sci. USA.* 109:3359–3364. https://doi.org/10.1073/pnas.1115967109

Beyer, E.C., and V.M. Berthoud. 2014. Connexin hemichannels in the lens. *Front. Physiol.* 5:20. https://doi.org/10.3389/fphys.2014.00020

Bhatnagar, A., N.H. Ansari, L. Wang, P. Khanna, C. Wang, and S.K. Srivastava. 1995. Calcium-mediated disintegrative globulization of isolated ocular lens fibers mimics cataractogenesis. *Exp. Eye Res.* 61:303–310. https://doi.org/10.1016/S0014-4835(05)80125-3

Braakhuis, A.J., C.I. Donaldson, J.C. Lim, and P.J. Donaldson. 2019. Nutritional Strategies to Prevent Lens Cataract: Current Status and Future Strategies. *Nutrients.* 11:1186. https://doi.org/10.3390/nu11051186

Burra, S., D.P. Nicolella, W.L. Francis, C.J. Freitas, N.J. Mueschke, K. Poole, and J.X. Jiang. 2010. Dendritic processes of osteocytes are mechanotransducers that induce the opening of hemichannels. *Proc. Natl. Acad. Sci. USA.* 107:13648–13653. https://doi.org/10.1073/pnas.1009382107

Cheng, B., Y. Kato, S. Zhao, J. Luo, E. Sprague, L.F. Bonewald, and J.X. Jiang. 2001. PGE(2) is essential for gap junction-mediated intercellular communication between osteocyte-like MLO-Y4 cells in response to mechanical strain. *Endocrinology.* 142:3464–3473. https://doi.org/10.1210/endo.142.8.8338

Davies, P.D., G. Duncan, P.B. Pynsent, D.L. Arber, and V.A. Lucas. 1984. Aqueous humour glucose concentration in cataract patients and its

effect on the lens. *Exp. Eye Res.* 39:605–609. https://doi.org/10.1016/0014-4835(84)90060-5

Davis, M.J., X. Wu, T.R. Nurkiewicz, J. Kawasaki, G.E. Davis, M.A. Hill, and G.A. Meininger. 2001. Integrins and mechanotransduction of the vascular myogenic response. *Am. J. Physiol. Heart Circ. Physiol.* 280: H1427–H1433. https://doi.org/10.1152/ajpheart.2001.280.4.H1427

Donaldson, P., J. Kistler, and R.T. Mathias. 2001. Molecular solutions to mammalian lens transparency. *News Physiol. Sci.* 16:118–123.

Donaldson, P.J., L.S. Musil, and R.T. Mathias. 2010. Point: A critical appraisal of the lens circulation model--an experimental paradigm for understanding the maintenance of lens transparency? *Invest. Ophthalmol. Vis. Sci.* 51:2303–2306. https://doi.org/10.1167/iovs.10-5350

Ebihara, L., J.-J. Tong, B. Vertel, T.W. White, and T.-L. Chen. 2011. Properties of connexin 46 hemichannels in dissociated lens fiber cells. *Invest. Ophthalmol. Vis. Sci.* 52:882–889. https://doi.org/10.1167/iovs.10-6200

Eskandari, S., G.A. Zampighi, D.W. Leung, E.M. Wright, and D.D. Loo. 2002. Inhibition of gap junction hemichannels by chloride channel blockers. *J. Membr. Biol.* 185:93–102. https://doi.org/10.1007/s00232-001-0115-0

Fasciani, I., A. Temperán, L.F. Pérez-Atencio, A. Escudero, P. Martínez-Montero, J. Molano, J.M. Gómez-Hernández, C.L. Paino, D. González-Nieto, and L.C. Barrio. 2013. Regulation of connexin hemichannel activity by membrane potential and the extracellular calcium in health and disease. *Neuropharmacology.* 75:479–490. https://doi.org/10.1016/j.neuropharm.2013.03.040

Fischbarg, J., F.P. Diecke, K. Kuang, B. Yu, F. Kang, P. Iserovich, Y. Li, H. Rosskothen, and J.P. Koniarek. 1999. Transport of fluid by lens epithelium. *Am. J. Physiol.* 276:C548–C557. https://doi.org/10.1152/ajpcell.1999.276.3.C548

Gangalum, R.K., D. Kim, R.K. Kashyap, S. Mangul, X. Zhou, D. Elashoff, and S.P. Bhat. 2018. Spatial Analysis of Single Fiber Cells of the Developing Ocular Lens Reveals Regulated Heterogeneity of Gene Expression. *iScience.* 10:66–79. https://doi.org/10.1016/j.isci.2018.11.024

Giblin, F.J. 2000. Glutathione: a vital lens antioxidant. *J. Ocul. Pharmacol. Ther.* 16:121–135. https://doi.org/10.1089/jop.2000.16.121

Jeong, B.Y., K.H. Cho, K.J. Jeong, Y.-Y. Park, J.M. Kim, S.Y. Rha, C.G. Park, G.B. Mills, J.-H. Cheong, and H.Y. Lee. 2018. Rab25 augments cancer cell invasiveness through a β1 integrin/EGFR/VEGF-A/Snail signaling axis and expression of fascin. *Exp. Mol. Med.* 50:e435. https://doi.org/10.1038/emm.2017.248

Jiang, J.X. 2001. Use of retroviruses to express connexins. *Methods Mol. Biol.* 154:159–174.

Jiang, J.X. 2010. Gap junctions or hemichannel-dependent and independent roles of connexins in cataractogenesis and lens development. *Curr. Mol. Med.* 10:851–863. https://doi.org/10.2174/156652410793937750

Jiang, J.X., and D.A. Goodenough. 1996. Heteromeric connexons in lens gap junction channels. *Proc. Natl. Acad. Sci. USA.* 93:1287–1291. https://doi.org/10.1073/pnas.93.3.1287

Jiang, J.X., and D.A. Goodenough. 1998. Retroviral expression of connexins in embryonic chick lens. *Invest. Ophthalmol. Vis. Sci.* 39:537–543.

Jiang, J.X., D.L. Paul, and D.A. Goodenough. 1993. Posttranslational phosphorylation of lens fiber connexin46: a slow occurrence. *Invest. Ophthalmol. Vis. Sci.* 34:3558–3565.

Jiang, J.X., T.W. White, D.A. Goodenough, and D.L. Paul. 1994. Molecular cloning and functional characterization of chick lens fiber connexin 45.6. *Mol. Biol. Cell.* 5(3):363–373. . https://doi.org/10.1091/mbc.5.3.363

Jiang, J.X., T.W. White, and D.A. Goodenough. 1995. Changes in connexin expression and distribution during chick lens development. *Dev. Biol.* 168:649–661. https://doi.org/10.1006/dbio.1995.1109

Katsumi, A., A.W. Orr, E. Tzima, and M.A. Schwartz. 2004. Integrins in mechanotransduction. *J. Biol. Chem.* 279:12001–12004. https://doi.org/10.1074/jbc.R300038200

Kinoshita, J.H. 1965. Pathways of glucose metabolism in the lens. *Invest. Ophthalmol.* 4:619–628.

Kuck, J.F. Jr. 1965. Carbohydrates of the lens in normal and precataractous states. *Invest. Ophthalmol.* 4:638–642.

Mathias, R.T., J. Kistler, and P. Donaldson. 2007. The lens circulation. *J. Membr. Biol.* 216:1–16. https://doi.org/10.1007/s00232-007-9019-y

Mathias, R.T., T.W. White, and X. Gong. 2010. Lens gap junctions in growth, differentiation, and homeostasis. *Physiol. Rev.* 90:179–206. https://doi.org/10.1152/physrev.00034.2009

Menko, A.S., K.A. Klukas, and R.G. Johnson. 1984. Chicken embryo lens cultures mimic differentiation in the lens. *Dev. Biol.* 103:129–141. https://doi.org/10.1016/0012-1606(84)90014-9

Michael, R., and A.J. Bron. 2011. The ageing lens and cataract: a model of normal and pathological ageing. *Philos. Trans. R. Soc. Lond. B Biol. Sci.* 366:1278–1292. https://doi.org/10.1098/rstb.2010.0300

Nguyen, D.H., T. Zhou, J. Shu, and J. Mao. 2013. Quantifying chromogen intensity in immunohistochemistry via reciprocal intensity. *Cancer InCytes.* 2:1–4.

Niu, J., T. Li, C. Yi, N. Huang, A. Koulakoff, C. Weng, C. Li, C.-J. Zhao, C. Giaume, and L. Xiao. 2016. Connexin-based channels contribute to metabolic pathways in the oligodendroglial lineage. *J. Cell Sci.* 129: 1902–1914. https://doi.org/10.1242/jcs.178731

Primo, L., G. Seano, C. Roca, F. Maione, P.A. Gagliardi, R. Sessa, M. Martinelli, E. Giraudo, L. di Blasio, and F. Bussolino. 2010. Increased expression of α6 integrin in endothelial cells unveils a proangiogenic role for basement membrane. *Cancer Res.* 70:5759–5769.

Retamal, M.A., N. Froger, N. Palacios-Prado, P. Ezan, P.J. Sáez, J.C. Sáez, and C. Giaume. 2007. Cx43 hemichannels and gap junction channels in astrocytes are regulated oppositely by proinflammatory cytokines released from activated microglia. *J. Neurosci.* 27:13781–13792. https://doi.org/10.1523/JNEUROSCI.2042-07.2007

Riquelme, M.A., S. Burra, R. Kar, P.D. Lampe, and J.X. Jiang. 2015. MAPK activated by prostaglandin E2 phosphorylates connexin 43 and closes osteocytic hemichannels in response to continuous flow shear stress. *J. Biol. Chem.* 290:28321–28328.

Ross, T.D., B.G. Coon, S. Yun, N. Baeyens, K. Tanaka, M. Ouyang, and M.A. Schwartz. 2013. Integrins in mechanotransduction. *Curr. Opin. Cell Biol.* 25:613–618. https://doi.org/10.1016/j.ceb.2013.05.006

Shi, W., M.A. Riquelme, S. Gu, and J.X. Jiang. 2018. Connexin hemichannels mediate glutathione transport and protect lens fiber cells from oxidative stress. *J. Cell Sci.* 131:jcs212506. https://doi.org/10.1242/jcs.212506

Slavi, N., C. Rubinos, L. Li, C. Sellitto, T.W. White, R. Mathias, and M. Srinivas. 2014. Connexin 46 (cx46) gap junctions provide a pathway for the delivery of glutathione to the lens nucleus. *J. Biol. Chem.* 289:32694–32702. https://doi.org/10.1074/jbc.M114.597898

Srinivas, M. 2014. Delivery of glutathione to the lens nucleus. *J. Ophthalmic Vis. Res.* 9:148–149.

Srinivasan, S., D.A. Weimer, S.C. Agans, S.D. Bain, and T.S. Gross. 2002. Low-magnitude mechanical loading becomes osteogenic when rest is inserted between each load cycle. *J. Bone Miner. Res.* 17:1613–1620. https://doi.org/10.1359/jbmr.2002.17.9.1613

Sun, Z., S.S. Guo, and R. Fässler. 2016. Integrin-mediated mechanotransduction. *J. Cell Biol.* 215:445–456. https://doi.org/10.1083/jcb.201609037

Swarup, A., B.A. Bell, J. Du, J.Y.S. Han, J. Soto, E.D. Abel, A. Bravo-Nuevo, P.G. FitzGerald, N.S. Peachey, and N.J. Philp. 2018. Deletion of GLUT1 in mouse lens epithelium leads to cataract formation. *Exp. Eye Res.* 172: 45–53. https://doi.org/10.1016/j.exer.2018.03.021

Trexler, E.B., F.F. Bukauskas, M.V. Bennett, T.A. Bargiello, and V.K. Verselis. 1999. Rapid and direct effects of pH on connexins revealed by the connexin46 hemichannel preparation. *J. Gen. Physiol.* 113:721–742. https://doi.org/10.1085/jgp.113.5.721

Tsuchida, J., S. Ueki, Y. Saito, and J. Takagi. 1997. Classification of 'activation' antibodies against integrin β1 chain. *FEBS Lett.* 416:212–216. https://doi.org/10.1016/S0014-5793(97)01206-4

Walker, J., and A.S. Menko. 2009. Integrins in lens development and disease. *Exp. Eye Res.* 88:216–225. https://doi.org/10.1016/j.exer.2008.06.020

Walker, J.L., L. Zhang, J. Zhou, M.J. Woolkalis, and A.S. Menko. 2002. Role for α 6 integrin during lens development: Evidence for signaling through IGF-1R and ERK. *Dev. Dyn.* 223:273–284. https://doi.org/10.1002/dvdy.10050

Wang, K., S. Gu, X. Yin, S.T. Weintraub, Z. Hua, and J.X. Jiang. 2012. Developmental truncations of connexin 50 by caspases adaptively regulate gap junctions/hemichannels and protect lens cells against ultraviolet radiation. *J. Biol. Chem.* 287:15786–15797. https://doi.org/10.1074/jbc.M111.313171

Webb, K.F., B.R. Merriman-Smith, J.K. Stobie, J. Kistler, and P.J. Donaldson. 2004. Cl- influx into rat cortical lens fiber cells is mediated by a Cl-conductance that is not ClC-2 or -3. *Invest. Ophthalmol. Vis. Sci.* 45: 4400–4408. https://doi.org/10.1167/iovs.04-0205

Whitson, J.A., D.R. Sell, M.C. Goodman, V.M. Monnier, and X. Fan. 2016. Evidence of dual mechanisms of glutathione uptake in the rodent lens: a novel role for vitreous humor in lens glutathione homeostasis. *Invest. Ophthalmol. Vis. Sci.* 57:3914–3925. https://doi.org/10.1167/iovs.16-19592

Yin, X., S. Gu, and J.X. Jiang. 2001. The development-associated cleavage of lens connexin 45.6 by caspase-3-like protease is regulated by casein kinase II-mediated phosphorylation. *J. Biol. Chem.* 276:34567–34572. https://doi.org/10.1074/jbc.M106073200

Zou, C., Y. Wang, and Z. Shen. 2005. 2-NBDG as a fluorescent indicator for direct glucose uptake measurement. *J. Biochem. Biophys. Methods.* 64: 207–215. https://doi.org/10.1016/j.jbbm.2005.08.001

Supplemental material

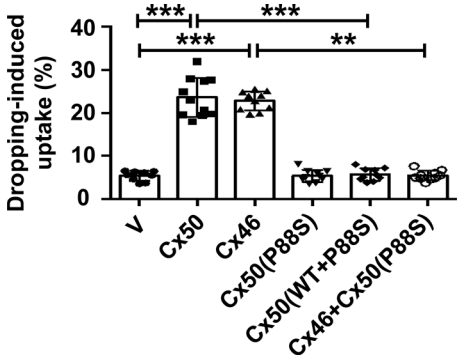

Figure S1. **Fluid dropping from a fixed distance has a mechanical stimulation effect comparable to that of FFSS.** CEF cells were infected with high-titer recombinant RCAS(A) retroviruses containing Cx50, Cx46, or P88S or coinfected retroviruses containing P88S and Cx50 or Cx46. Mechanical stimulation was applied by dropping the medium from a fixed distance. LY/RD dye uptake was conducted after mechanical stimulation. The percentage of cells with LY dye uptake (excluding cells that took up both LY and RD-dextran) was quantified. Each data point in the graph represents an individual quantified image. Data are presented as mean ± SEM. **, P < 0.01; ***, P < 0.001.

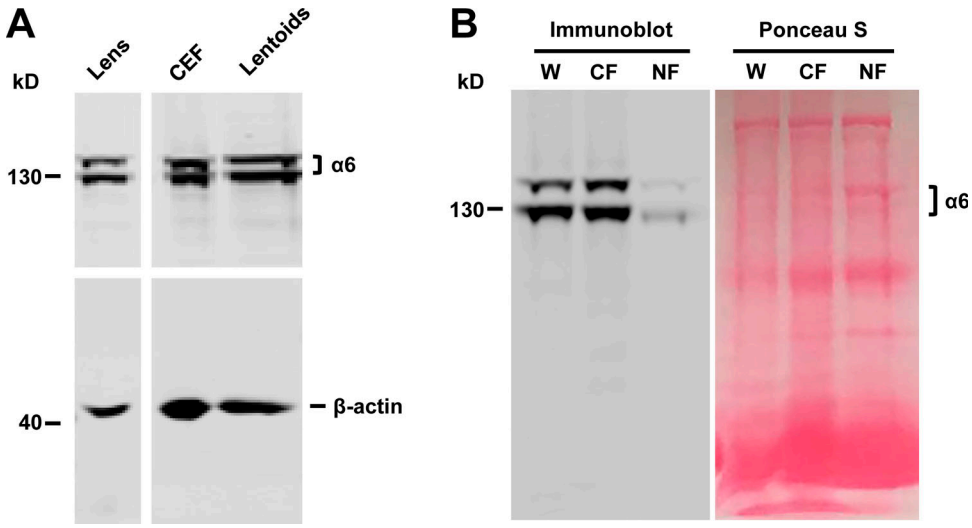

Figure S2. **Integrin α6 is expressed in cortical lens, primary chick lens culture, and CEF cells. (A)** Crude membrane extracts were prepared from whole chick lens, CEF cells, and differentiated primary chick lens culture containing lentoids and immunoblotted with anti-integrin α6 antibody and β-actin antibody. **(B)** Crude membrane extracts were prepared from whole chick lens (W) or isolated E18 chick lens portions containing cortical fibers (CF) or nuclear fibers (NF). Integrin α6 was detected in the cortical lens fibers, but not in the central, nuclear lens fiber. As no actin was expressed in nuclear lens, Ponceau S staining was used to show that a comparable amount of protein was loaded on SDS-PAGE.

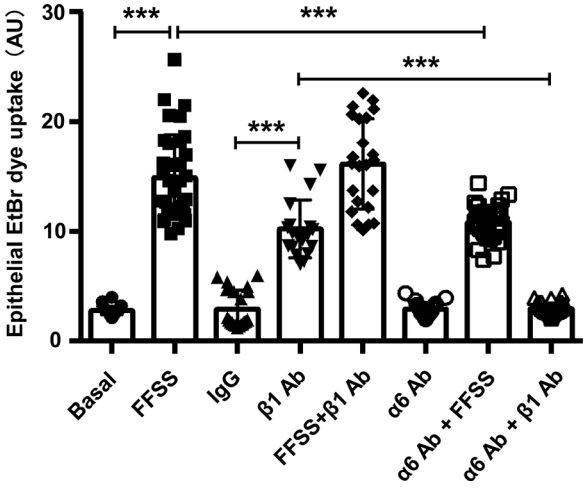

Figure S3. **Hemichannel opening by FFSS is regulated by integrin α6β1 in lens epithelial cells.** Primary chick lens culture was pretreated with or without integrin α6 blocking antibody (α6 Ab) at 10 µg/ml for 1 h, then subjected to FFSS at 1 dyn/cm^2 for 10 min or treated with β1 Ab at 20 µg/ml for 1 h separately or in combination, followed by EtBr/FITC dye uptake assay. FITC-dextran (M_r 10 kD) was used as a control for nonspecific membrane permeability (dying cells). The monolayer epithelial cells were imaged, and the level of EtBr uptake was quantified with EtBr dye uptake (excluding cells that took up both EtBr and FITC-dextran) using ImageJ. Each data point in the graph represents an individual quantified epithelial cell in one of three independent experiments. The data are presented as mean ± SEM. ***, P < 0.001.

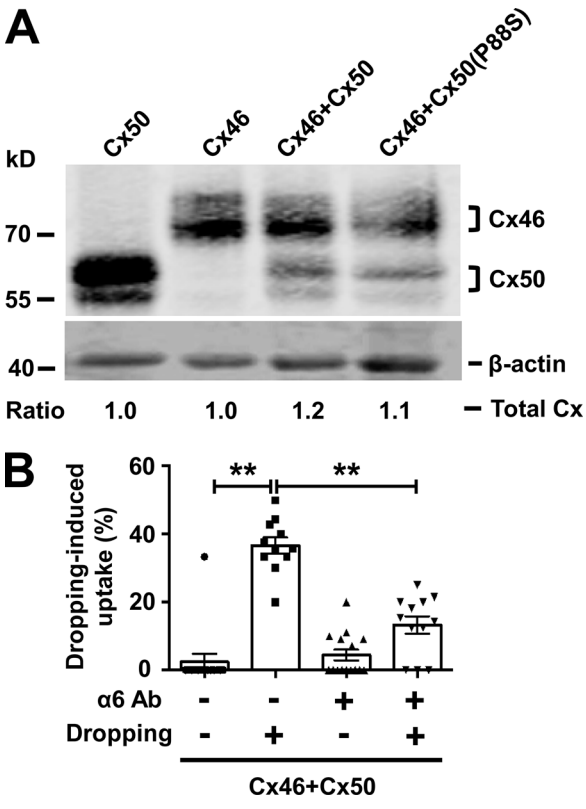

Figure S4. **Integrin α6 is required in mechanical loading–induced opening of heteromeric hemichannels formed by Cx50 and Cx46. (A)** CEF cells were infected with recombinant RCAS(A) retroviruses containing Cx50 or Cx46 or coinfected with retroviruses containing Cx46 with Cx50 or Cx50 mutant P88S. Crude cell membrane extracts were prepared and immunoblotted with anti-FLAG-tag and β-actin antibodies. The relative ratio of band intensity of total connexins (Cx50 and/or Cx46) to housekeeping protein β-actin with the ratio of the control setting as 1 is shown underneath the immunoblot. **(B)** The co-infected CEF cells expressing both Cx50 and Cx46 were pretreated with α6 Ab, followed by fluid dropping mechanical stimulation. LY/RD dye uptake assay was conducted, and the percentage of cells with LY dye uptake (excluding cells that took up both LY and RD-dextran) was quantified. Each data point in the graph represents an individual quantified image in one of three independent experiments. The data are presented as mean ± SEM. **, P < 0.01.

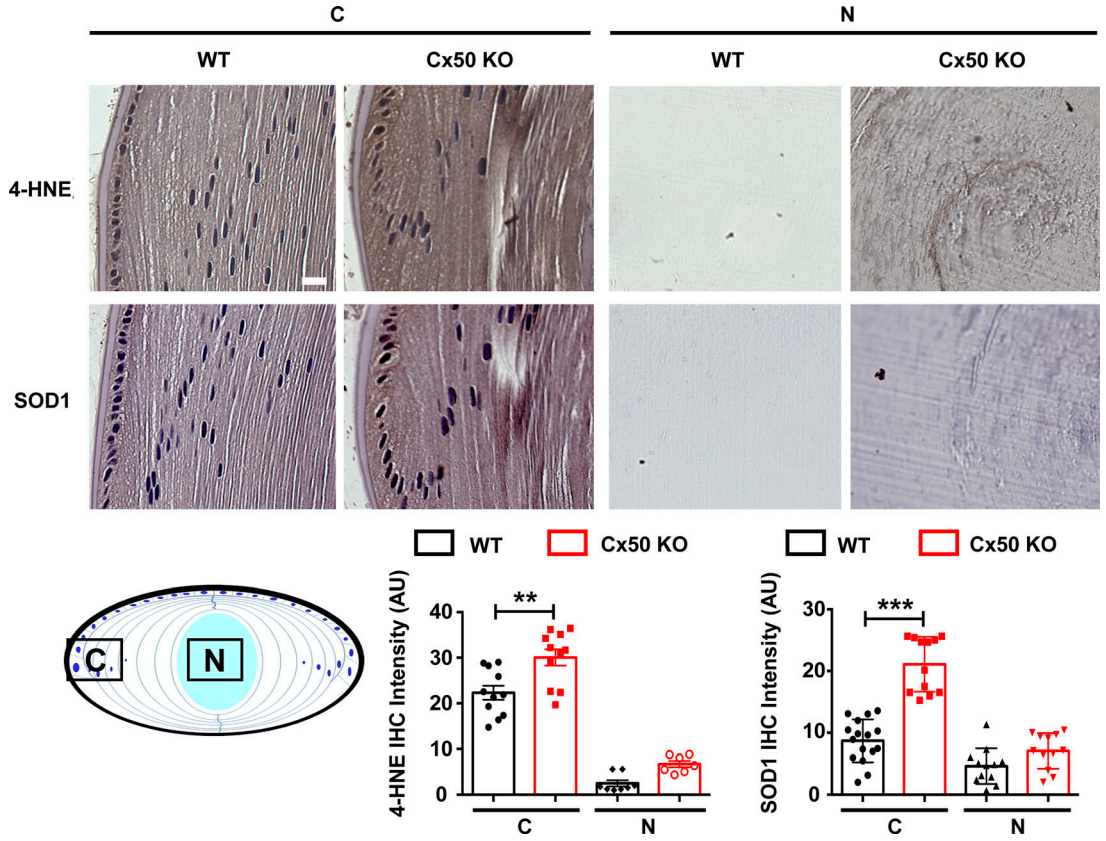

Figure S5. **Increased oxidative stress in the Cx50-deficient mouse lens.** Immunohistochemical staining with anti-4-HNE and anti-SOD1 antibodies was adopted to assess the oxidative stress level in WT and Cx50 KO mice lens. Sagittal paraffin sections of 2-mo-old mouse lenses from WT and Cx50 KO mice were prepared. The ABC (avidin–biotin–peroxidase complex) Immunostaining Assay Kit (PK-6101; Vector Laboratories) was used. Briefly, lens tissue sections were antigen unmasked using sodium citrate buffer (pH 6.0) at 65°C for 2 h for 4-HNE and SOD1 staining. Lens tissue sections were then treated with rabbit normal serum for 20 min at room temperature to block nonspecific staining. Tissue sections were stained with anti-4-HNE monoclonal antibody (1:150 dilution; ab46545; Abcam) or anti-SOD1 antibody (1:200 dilution; SC11407; Santa Cruz) for 30 min at room temperature. The sections were then incubated for 30 min with biotin-labeled secondary antibody and VECTASTAIN ABC Reagent for 30 min. Samples were washed in PBS and developed in DAB (SK4100) chromogen solution (Vector Laboratories). Tissues were then counterstained with Hematoxylin (H-3401; Vector Laboratories) for 5 min at room temperature and mounted. Sections were photographed using a Keyence microscope (BZ-X710). The expression level of 4-HNE and SOD1 (brown signals, upper panel) in the cortical lens (C) and nuclear lens (N) was quantified using ImageJ, and reciprocal intensity (Nguyen et al., 2013) is displayed (lower panel). Each data point in the graph represents an individual quantified region in one of three independent experiments. Scale bar, 20 µm. The data are presented as mean ± SEM. **, $P < 0.01$; ***, $P < 0.001$.